Since January 2020 Elsevier has created a COVID-19 resource centre with free information in English and Mandarin on the novel coronavirus COVID-19. The COVID-19 resource centre is hosted on Elsevier Connect, the company's public news and information website.

Novel hit of DPP-4Is as promising antihyperglycemic agents with dual antioxidant/anti-inflammatory effects for type 2 diabetes with/without COVID-19

Shahenda Mahgoub [a,*], Samar S. Fatahala [b,*], Amira I. Sayed [b], Hanaa B. Atya [a],
Mohamed F. El-Shehry [c], Hala Afifi [d,e], Samir M. Awad [b], Rania H. Abd El-Hameed [b], Heba Taha [a]

[a] Department of Biochemistry and Molecular Biology, Faculty of Pharmacy, Helwan University, Helwan, Cairo 11795, Egypt
[b] Pharmaceutical Organic Chemistry Department, Helwan University, P.O. Box 11795, Helwan, Cairo, Egypt
[c] Pesticide Chemistry Department, National Research Centre, P.O. Box 12622, Dokki, Egypt
[d] Department of Pharmaceutical Chemistry, Faculty of Pharmacy, Ain-Shams University, Egypt
[e] Department of Pharmacy, City University College of Ajman, UAE

ARTICLE INFO

ABSTRACT

DPP-4Is are well recognized therapy for type 2 diabetes. In spite of sharing a common mode of action, the chemical diversity among members of DPP-4Is raised the question whether structural differences may result in distinguished activities. DPP-4Is were recently explored as drug repurposing means for treatment of SARS-CoV-2 due to the urgent need for small molecule drugs for controlling infections. The use of DPP-4Is was not correlated with adverse COVID-19-related consequences among patients with type 2 diabetes. Inspired by these reasons and the importance of pyrimidinone ring as DPP-4I with both antioxidant and anti-inflammatory activities, we succeeded to prepare some novel pyrimidinone and thio-pyrimidinone derivatives, which were then screened for their antidiabetic activity and DPP-4 inhibition. In addition, their anti-inflammatory effect on LPS-stimulated RAW 264.7 cells were evaluated. Furthermore, their antioxidant activities were also tested.

1. Introduction

Diabetes mellitus (DM) is an endocrine disorder which is characterized by hyperglycemia, polydipsia, and polyuria as a result of a defect in insulin secretion and/or action. It is associated with metabolic, microvascular and macrovascular complications that increase morbidity and mortality in various viral infections [1]. DM and reactive hyperglycemia are considered as predictors of severity in severe acute respiratory syndrome coronavirus (SARS-CoV) and Middle East respiratory syndrome coronavirus (MERS-CoV) infected patients [2] and several studies showed a link between hyperglycemia and severe acute respiratory syndrome coronavirus 2 (SARS-CoV-2) even in non-diabetic patients [3]. Diabetes is considered as one of the most important comorbidities in SARS-CoV-2 infected patients and the incidence of diabetes in those patients ranged from 5% to 36% [4]. Moreover, diabetes accounted for nearly 20% of the intensive care unit admitted cases due to coronavirus disease 2019 (COVID-19) [5]. SARS-CoV-2 which is responsible for COVID-19, utilizes angiotensin-converting enzyme 2 (ACE2) to enter human cells. However, recent evidence proposed that dipeptidyl peptidase-4 (DPP-4) may be used as a co-receptor for SARS-CoV-2 to enter the target cells [6] and that SARS-CoV-2 interacts with DPP-4/CD26 and the 293 T-cells expressing DPP-4 [7], which was also suggested by modelling studies [8]. DPP-4 is a type II transmembrane glycoprotein. It is expressed in several tissues and immune cells with higher expression in the visceral adipose tissue. DPP-4 is also present on the endothelial cells of blood vessels and circulates in a soluble form in blood plasma thus, it regulates blood hormones. DPP-4 plays a crucial role in the metabolism of glucagon-like peptide-1 (GLP-1) and it is involved in visceral inflammation as well as the development of insulin resistance [9], in addition to its immunomodulatory effects [10]. Moreover, it was found that the soluble DPP-4 rises the inducible nitric oxide synthase (iNOS) expression and the production of proinflammatory cytokines in lipopolysaccharide (LPS) stimulated macrophages, besides the stimulation of ROS production and the activation of the advanced glycation end products gene expression [11,12]. Furthermore, up-regulation of DPP-4 is linked with elder age, diabetes,

obesity, and metabolic syndrome, as well as, respiratory and cardio-vascular diseases, which were reported to aggravate COVID-19 [10].

DPP-4 inhibitors (DPP-4Is) or gliptins have been used for treatment of type 2 diabetes mellitus (T2DM) since 2006. They are orally available small molecules that interact with the DPP-4 enzyme [13]. DPP-4Is have no intrinsic glucose-lowering activity, so their efficacy; as anti-diabetic agents; is related to their ability to inhibit DPP-4 activity thus, increasing the incretin levels, which, subsequently, increases insulin secretion and reduces blood glucose levels (BGLs) with no risk of hypoglycemia [14]. Also, DPP-4Is exhibited anti-inflammatory and immunoregulatory activities in the autoimmune and inflammatory disorders [15]. Previous studies have disclosed that the principal clinical approach for DPP-4Is with antioxidant abilities involves the front-line treatment, due to their safety, and tolerability since DPP-4Is with their antioxidant capability can affect the immune system and its function [16]. It was found that the use of DPP-4Is was not correlated with adverse COVID-19-related consequences among patients with T2DM [17]. Additionally, a study by *Mirani et al.* showed that diabetic patients on DPP-4I therapy developed a less severe pneumonia, with a lower need for mechanical ventilation and a lesser mortality rate on developing COVID-19, indicating that DPP-4Is reduce COVID-19 virulence through the suppression of DPP-4/CD26-dependent inflammatory signaling with subsequent inhibition of cytokine storm and disease progression [18]. Likewise, gliptins can inhibit SARSCoV-2 proliferation through their binding to the F357 residue, causing conformational changes that inhibit the viral binding to DPP-4 receptors [8].

Due to the urgent need for drugs to control COVID-19, small molecule drugs still establish a worthwhile treatment for controlling infections. Yet, discovering new drugs is usually a time consuming and expensive progress over the idea of drug repurposing, which provides a rapid therapy with proven record of safety and efficacy [16,19].

Since increased DPP-4 expression and activity are associated with diabetes, obesity and metabolic syndrome, and if DPP4 expression facilitates infection by SARS-CoV-2, therefore, DPP-4Is may be used to treat COVID-19 patients with raised BGLs and/or markers of viral infection induced hyper-inflammation [20] to mitigate diabetes and coexisting COVID-19-induced insulin resistance, hyperglycemia, and inflammation [10].

2. Results and discussion

2.1. Chemistry

Literature survey was performed to understand the history and chemistry of gliptins, the new oral antidiabetic agents, which were discovered for being DPP-4Is, from these approved DPP-4Is; sitagliptin, vildagliptin, saxagliptin, alogliptin and anagliptin, (Fig. 1). Yet, to understand the chemistry and mode of action of gliptins, the structure of DPP-4 and its substrates should be mentioned and studied [21,22].

DPP-4 is a prolyl-specific protease, namely, a homodimeric serine peptidase (or a dimer of dimers for the whole enzyme) that regulates the structure of bioactive peptides (the substrate) with Pro or Ala at the *N*-terminal penultimate position (P-residues). Among the former substrates, glucagon-like peptide-1 (GLP-1), which is degraded by DPP-4 enzyme.

To understand the way the enzyme interacts with the peptide substrate, a deeper look is required in the structure of DPP-4. It consists of approximately 766 amino acids in each subunit, with a large active site consisting of multiple binding subsites known as the S1, S2, S1′ and S2′ extensive subsites. Each subunit comprises a C-terminal α/β hydrolase domain and an *N*-terminal, β-propeller domain [23]. The cleavage residue of a substrate peptide consists of *P2*, *P1*, *P1′*, and *P2′* according to the protease subsites S2, S1, S1′, and S2′ that they interact with, (Fig. 2). The cleavage site of the peptide substrate is *N*-terminus that typically
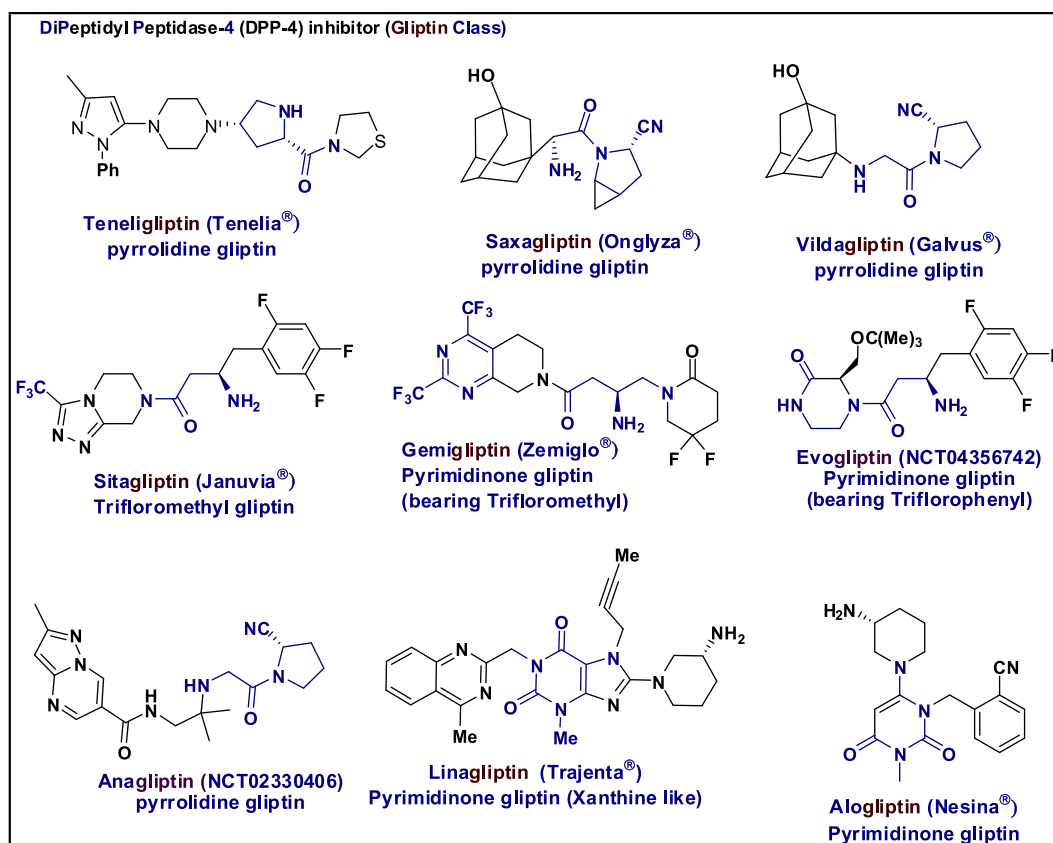

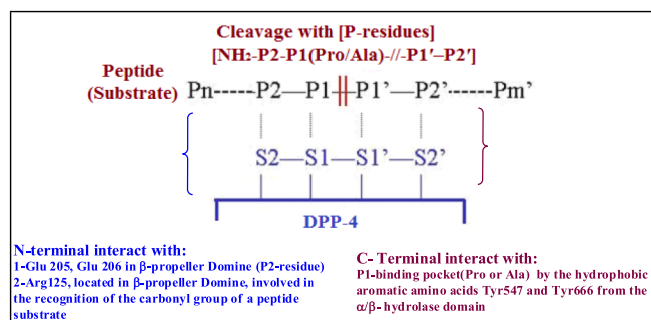**Fig. 1.** Approved DPP-4Is classified according to the main structures.

Fig. 2. Schematic representation for DPP-4/Substrate complex.

have a proline (Pro) or an alanine (Ala) residue in the penultimate position between *P*1 and *P*1′ residues, while the *P*2 position of *N*-terminus of the peptide substrate acts as the recognition region [22,24–31].

Recently, analyzing and understanding the structure activity relationship (SAR) of DPP-4Is revealed that the most important residues responsible for DPP-4 inhibition are the hydrophobic S1 pocket residues, catalytic triad residues, *N*-terminal recognition region residues (*P*1 & *P*2) and hydrophobic S2 pocket residues [23]. Gliptin-like structure as sitagliptin, vildagliptin, saxagliptin, alogliptin and anagliptin, the approved DPP-4Is (Fig. 1), can be classified referring to their structures and enzyme inhibition mechanism into three main groups [21]. First, those with (i) pyrrolidine or analogues with α-aminoacyl linker to S1 subunit of the enzyme & *P*1 residues of substrates; as in vildagliptin, saxagliptin and teneligliptin. These cyano-pyrrolidines or thiazolidines can form both H-bonding and hydrophobic interaction with S1, S2 and *P*1, *P*2 extensive domains. (ii) trifluoro bearing structures (trifloromethyl, trifluorophenyl or difluoropiperidone) as in sitagliptin, evogliptin and gemigliptin, with β-aminobutanoyl linker, having the ability to bind to S1 pocket of the enzyme and *P*1 residues of substrate, through fluorine and β-aminobutanoyl forming H-bonding, in addition to hydrophobic interaction with the aromatic amino acids. (iii) pyrimidine-2,4-dione (as alogliptin, evagliptin, trelagliptin and linagliptin) form a salt bridge interaction with S1, *P*1 pocket as well as *P*1′, S1′ pocket of the enzyme/substrate, providing H-bonding in addition to π-π interaction, which aids in more stability for the compounds in the active site, thus allowing high inhibitory effect, (Fig. 1).

Till now, for all these categorizations, the amino linkage is very important to form hydrogen bonds with the pocket, although modifications like replacing these amino linkers with more rigid analogue (as cyclohexylamine) provided more hydrophobic interactions with the side chain of amino acids of the enzyme. On the other hand, a number of

structural modifications have been made in order to increase DPP-4Is antidiabetic activity and minimize their well-known side effects [32–34]. Among these modifications, the identification of natural compounds as new DPP-4Is with fewer side effects. Herbal medicines for diabetic therapy are widely used, but with lower effective degree. Recently DPP-4 was selected as a field template to search for natural, small phenolic compounds as new DPP-4Is, namely, flavone, chrysin, luteolin, curcumin and resveratrol, which were found to have great affinity for DPP-4 enzyme through both electrostatic and hydrophobic interactions. Recently, the role of these naturally occurring phenolic compounds as antidiabetics (DPP-4Is) were also accompanied with their antioxidant, and anti-inflammatory effects, (Fig. 3).

Anagliptin, vildagliptin (pyrrolidine gliptin), as well as pyrimidinedione gliptin (linagliptin & alogliptin) are two groups of DPP-4Is having both anti-inflammatory and antioxidant activities, aside from their potent anti-diabetic effects, (Fig. 1). They inhibited the inflammatory and fibrotic gene expression in macrophages through decreasing the DPP-4 activity implicated in transforming growth factor (TGF) -mediated fibroblast activity (Anagliptin, Vildagliptin and linagliptin), and/or inhibiting the inflammatory responses by preventing the toll-like receptor 4 (TLR-4)-mediated formation of pro-inflammatory cytokines (Alogliptin) [35,36].

DPP-4Is were recently reconnoitered as drug repurposing route for treatment of SARS-CoV-2 infections, due to an urgent need for small molecule drugs for controlling infections. Three pyrimidinone gliptin namely, gemigliptin, linagliptin and evogliptin, are being investigated as broad-spectrum antiviral agents, for their effects as potential inhibitors of viral cysteine protease in both SARS & MERS [19,37], (Fig. 1).

Inspired by all the above-mentioned motives along with the importance of pyrimidinone ring as DPP-4I bearing antioxidant and anti-inflammatory activities, which can aid in controlling the corona viruses, we succeeded to prepare some novel pyrimidinone and thio-pyrimidinone (**1**–**8**) which were screened for their antidiabetic and DPP-4 inhibition. Furthermore, their anti-inflammatory effect on LPS-stimulated RAW 264.7 cells and their antioxidant activity using DPPH assay were evaluated. Here, we developed a program for the synthesis and evaluation as designed in Fig. 4.

The lead compounds; our target compounds, the new pyrimidinone sulfonamide derivatives, were prepared through a two-step reaction. The first was by the reaction of 2-thiouracil with chlorosulfonic acid at 120°C to obtain 2-thiouracil-5-sulfonyl chloride (**2**). Compound **2** reacted in the second step with appropriate substituted urea or thiourea in basic medium to obtain sulfonamide derivatives (**3a-d**), which were used as starting materials for the synthesis of new pyrimidine
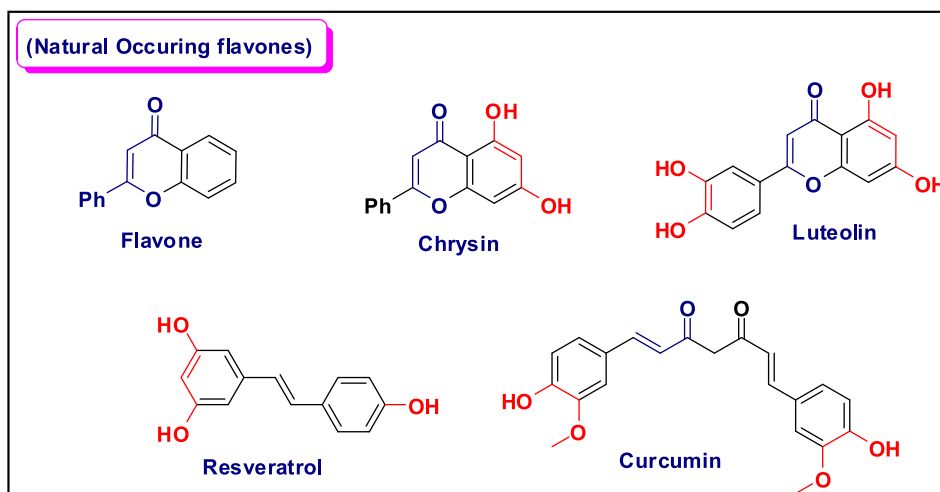

Fig. 3. Naturally occurring phenolic compounds having DPP-4 inhibition potent activity.
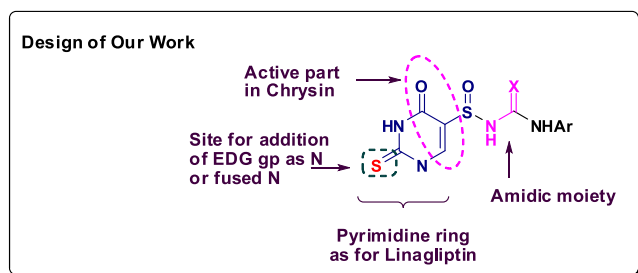
Fig. 4. Aim of our work.

sulfonamide derivatives [38–40].

Reaction of thiouracil derivatives with halogenated compounds in basic medium to produce S-alkylated derivatives was reported [41,42]. On the basics of this previously reported reactions; thiouracil derivatives **3a-d** were successfully alkylated with chloroacetic acid in the presence of sodium hydroxide to afford sulfanyl acetic acid derivatives **5a-d**. Furthermore, the reaction of **3a-d** with chloroacetyl chloride in the presence of triethyl amine not only caused S-alkylation but led to internal cyclisation to afford thiazolo [3,2-a] pyrimidine derivatives **4a-d** [43]. Heating under reflux of compounds **3a-d**, separately, with hydrazine hydrate gave the corresponding 2-hydrazion-pyrimidine derivatives **6a-d** in fair yields [44], as revealed in Scheme 1.

2.2. Biological evaluation

#### 2.2.1. Evaluation of the antihyperglycemic activity

The burden of T2DM is growing globally with equal gender distribution and 55 years of age incidence peaks. Moreover, the prevalence of T2DM is expected to increase globally by the year 2030 to reach 7079 per 100,000 individuals, which reflects a sustained increase in the number of type 2 diabetic patients all over the world [45].

T2DM is characterized by a prolonged hyperglycemia caused by a combination of insulin tolerance in muscles and liver, and decreased insulin production by the beta cells of the pancreas [46,47]. Chronic hyperglycemia, microvascular and macrovascular complications associated with T2DM significantly increase disease-associated morbidity and mortality. Moreover, epidemiologic data showed that diabetic patients are at higher risk of developing various diseases like cardiovascular, musculoskeletal, and psychiatric disorders [48–50].

Recently, a growing number of studies have shown that T2DM is the comorbidity with the greatest negative impact on the prognosis of patients with COVID-19. Type 2 diabetic patients who get COVID-19 are more likely to develop severe COVID-19 and have higher mortality rates [51,52]. Consequently, several newer approaches with novel mode of action have been emerged to improve T2DM management. The collision of these two major global epidemics urges the correct use of the antidiabetic agents. Since DPP-4Is are commonly used antihyperglycemics, thus, the relationship between DPP-4Is use and COVID-19 has also attracted increasing attention.

Hence our study started with the *in vivo* screening of all synthesized compounds (**3–8**) for their potential antihyperglycemic effect using the oral glucose tolerance test (OGTT) utilizing diamicron as a reference standard. As depicted in Table 1., the antihyperglycemic effect was evident by the decrease in the glucose area under the curve (AUC) of the oral tolerance test when compared to the control rats. The most active compound was **4c,** which caused reduction in AUC by ~25% followed by **4b, 5a, 8c, 5c, 4d, 8b** and **6b,** which showed a close activity with
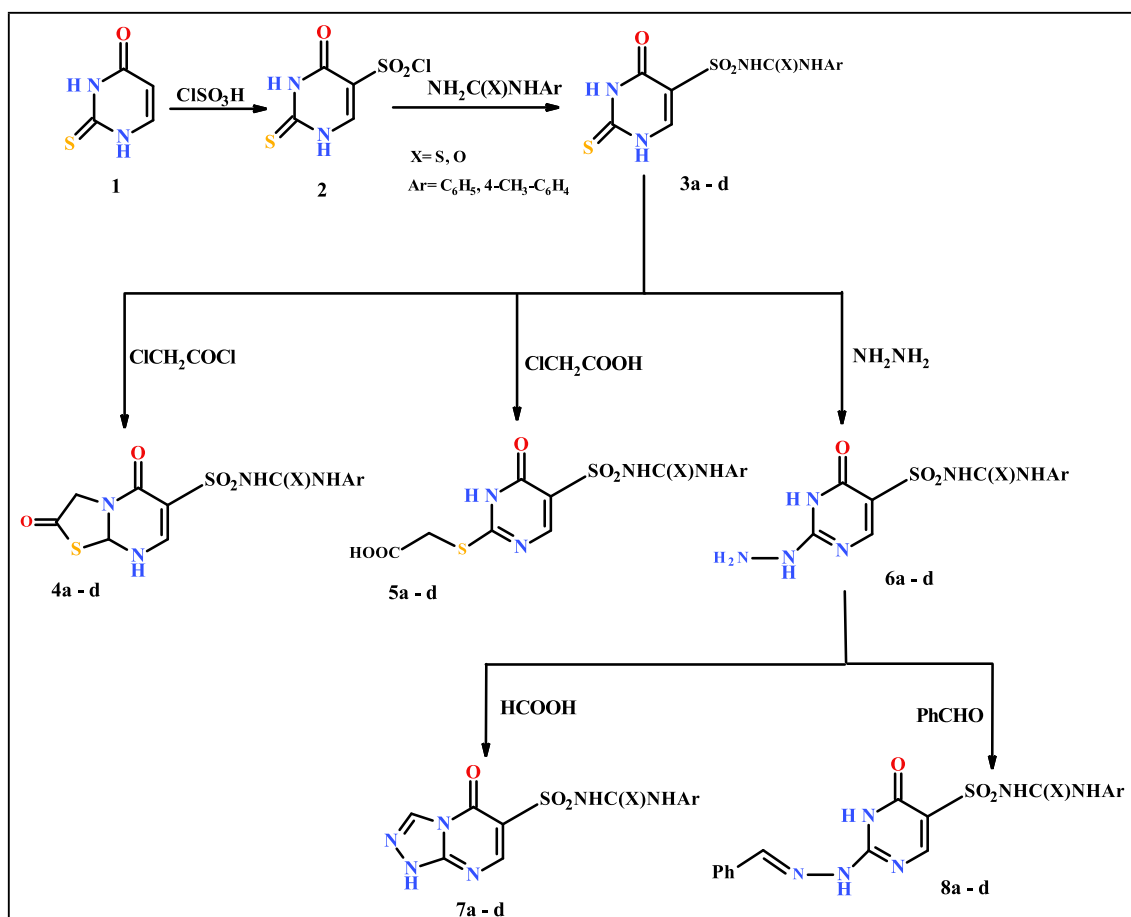
Scheme 1. Preparation of compounds (**1–8**).

Table 1
Screening the effect of various compounds oral administration on blood glucose levels in normal rats during an OGTT.

Compound	AUC (mg.min/dl)	% Reduction in BGL compared to control
3a	194.50 ± 23.83	NA
3b	242.50 ± 17.60	NA
3c	226.96 ± 15.08	NA
3d	215.95 ± 14.32	NA
4a	236.00 ± 21.56	NA
4b	173.71 ± 11.61 [***]	22.75
4c	168.00 ± 29.14 [***]	25.29
4d	181.50 ± 9.71 [**]	19.90
5a	176.04 ± 14.50 [***]	21.58
5b	189.14 ± 14.87 [*]	15.89
5c	181.75 ± 13.24 [**]	19.97
5d	193.83 ± 14.46	NA
6a	185.08 ± 20.62[*]	17.70
6b	182.75 ± 13.43[**]	18.73
6c	185.83 ± 8.16[*]	17.36
6d	195.67 ± 19.52	NA
7a	185.42 ± 19.64[*]	17.55
7b	191.79 ± 13.77	NA
7c	186.17 ± 8.62[*]	17.21
7d	186.29 ± 17.82[*]	17.16
8a	186.92 ± 16.21[*]	16.88
8b	182.00 ± 13.52[**]	19.07
8c	178.04 ± 14.15[***]	20.83
8d	221.63 ± 9.18	NA
Diamicron	189.21 ± 10.45[*]	15.86

Data is presented as mean AUC ± SD. * Significant (P < 0.05), ** (P < 0.01) or *** (P < 0.001) compared to control group. NA: Not active. N = 6. OGTT: oral glucose tolerance test.

~19–22% reduction in AUC. Moreover, compounds **6a, 6c, 7a, 7c, 7d** and **8a** showed promising activity and finally compound **5b.**

2.2.2. *In vitro screening of DPP-4 inhibition activity*

DPP-4Is; known as the gliptins; are a class of oral antidiabetics approved by the Food and Drug Administration (FDA) for treatment of T2DM. In addition to their antihyperglycemic effects, the gliptins have several activities independent of the incretin pathway like antihypertensive, anti-inflammatory, and immunomodulatory effects [53]. DPP-4 allocation in the human respiratory tract may help the SARS-CoV-2 entry. Moreover, it could contribute to the development of the hyper-inflammatory response and to the cytokine storm causing fatal pneumonia [6]. Similarly, SARS-CoV-2 infection may worsen the current DM and even more prompt to frank DM in non-diabetic patients [54]. Hence, the use of DPP-4Is may decrease the virus entry into the airways and may mitigate DM and coexisting COVID-19-induced insulin resistance, hyperglycemia, and inflammatory response [10].

Thus, the promising antihyperglycemic activity displayed by about 15 out of 24 tested compounds encouraged us to test their *in vitro* inhibitory activity against DPP-4 enzyme (using linagliptin as a positive control drug) in an attempt to find antihyperglycemic compounds with DPP-4 inhibition potency thus, mitigate the diabetic state and alleviate the hyperglycemic and inflammatory states induced by SARS-CoV-2 infection. Consequently, may have favorable effects on COVID-19 outcomes *via* decreasing the risk of greater COVID-19 severity and mortality in Type 2 diabetic patients. The results showed that five compounds depicted promising *in vitro* inhibitory activity against DPP-4 enzyme, Table 2. Compounds **6a** and **7d** showed the highest inhibitory activity (IC$_{50}$, 0.047 ± 0.002 and 0.057 ± 0.003 μM, respectively) followed by compound **4b** (IC$_{50}$, 0.063 ± 0.003). Compounds **6b** and **8b** showed strong inhibitory effect (IC$_{50}$, 0.071 ± 0.004 and 0.075 ± 0.003 μM, respectively) against the DPP-4 enzyme.

2.2.3. *Effect of the synthesized compounds on blood glucose levels and plasma DPP-4 activity in type 2 diabetic rats*

The high fat diet (HFD) was used in rats to induce insulin resistance,

Table 2
In vitro DPP-4 inhibitory activities of the selected test compounds.

Compound	DPP-4 IC$_{50}$ (μM)
4b	0.063 ± 0.003
4c	0.418 ± 0.020
4d	1.324 ± 0.065
5a	0.577 ± 0.028
5b	0.634 ± 0.031
5c	0.290 ± 0.018
6a	0.047 ± 0.002
6b	0.071 ± 0.004
6c	0.264 ± 0.013
7a	0.153 ± 0.008
7c	0.277 ± 0.014
7d	0.057 ± 0.003
8a	0.104 ± 0.005
8b	0.075 ± 0.003
8c	0.468 ± 0.023
Linagliptin	0.023 ± 0.001

Data is displayed as mean ± SD.

while the low streptozotocin (STZ) dose caused decrease in the ability of pancreatic cells to produce sufficient insulin levels and thus, T2DM was induced in rats, which was manifested by the significant increase in the AUC of OGTT. Then, the effect of the oral administration of the most active compounds at equivalent doses of 10 mg/kg on BGLs of the diabetic rats was investigated using linagliptin as a positive control drug. Compounds **4b, 6a, 6b, 7d** and **8b** significantly improved glucose tolerance. **4b, 6b** and **7d** showed the most potent effect followed by **6a** and **8b**, when compared to linagliptin, as shown by the marked reduction in the AUC of OGTT compared to the control diabetic group, (Table 3).

To evaluate the effect on plasma DPP-4 activity, linagliptin (10 mg/kg) and the five active compounds i.e., **4b, 6a, 6b, 7d** and **8b** at their equivalent doses were administered to the type 2 diabetic rats after an overnight fasting. As shown in Fig. 5, plasma DPP-4 activity was significantly decreased (p < 0.001) by compounds **4b, 7d**, and **6b** (by about 63, 57, and 53%, respectively), followed by compounds **8b** and **6a** (48 and 51%, respectively) and by 67% in linagliptin group, when compared to the vehicle treated control diabetic group.

2.2.4. *The anti-inflammatory effect of the synthetic derivatives*

DPP-4 regulates the local and systemic inflammation via cleavage of the immunomodulatory DPP-4 substrates [55,56]. DPP-4Is succeeded to

Table 3
Screening the effect of active compounds on BGLs during an OGTT in type2 diabetic rats.

Compound	AUC (mg.min/dl)	% Reduction in BGL compared to control
4b	496.33 ± 40.87[***]	36.59
4c	NA	NA
4d	NA	NA
5a	NA	NA
5b	NA	NA
6a	600.80 ± 71.47[***]	23.24
6b	461.79 ± 35.63[***]	41.00
6c	NA	NA
7a	NA	NA
7b	NA	NA
7c	NA	NA
7d	509.29 ± 54.66[***]	34.94
8a	NA	NA
8b	595.38 ± 50.23[***]	23.94
8c	NA	NA
Linagliptin	497.65 ± 55.15[***]	36.42

Data is presented as mean AUC ± SD. * Significant (P < 0.05), ** (P < 0.01) or *** (P < 0.001) compared to control group. OGTT: oral glucose tolerance test, NA: Not active. (N = 6).
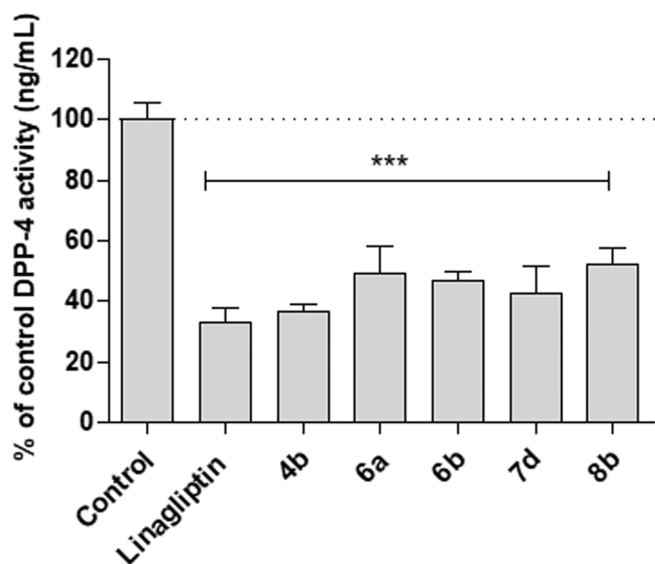
Fig. 5. *In vivo* **DPP-4 activity as % of control in type2 diabetic rats,** Values are mean ± SD (n = 3). ***significant (P < 0.001) compared to control diabetic group.

reduce inflammation in preclinical studies and in patients with T2DM [57]. It was reported that SARS-CoV, a closely related virus to SARS-CoV-2; can cause pancreatic β-cell function impairment and transient hyperglycemia [58]. Moreover, the COVID-19-induced inflammatory state and cytokine storm, which are characterized by the extreme release of tumor necrosis factor alpha (TNF-α) and interleukin (IL)-6; has led to peripheral insulin resistance [59]. Studies revealed that DPP-4 inhibition may alienate SARS–CoV-2 virulence and the subsequent multiorgan damage via several mechanisms that include decreasing the overproduction of cytokines [56,60]; reducing the activity of macrophages [61]; inducing direct pulmonary anti-inflammatory effects [62,63]; and finally augmenting GLP-1 anti-inflammatory activity [64,65], mainly in COVID-19 [6]. Inspired by these effects, we evaluated the potential anti-inflammatory effect of the compounds with the highest DPP-4 inhibition activities *viz* **4b, 6a, 6b, 7d,** and **8b**.

Macrophage cell lines are applied in numerous studies of inflammation [66]. Lipopolysaccharides (LPS) is commonly used to stimulate the macrophages in order to establish an inflammatory model [67,68]. Therefore, in our study we evaluated the effect of the selected compounds against the cytokine response of murine macrophage RAW 264.7 cells to LPS stimulation.

2.2.4.1. In vitro cytotoxicity of the selected derivatives against RAW264.7 cells. MTT assay was used to evaluate the effect of compounds **4b, 6a, 6b, 7d,** and **8b** on RAW264.7 macrophage cell viability at five concentrations i.e., 250, 63, 16, 4, and 1 μM without LPS. The results are shown in Table 4 and showed that all derivatives have IC$_{50}$ above 100 μM. Thus, all the compounds were used at concentrations equivalent to ¼ IC$_{50}$ for cytokine release evaluation in order to study their anti-inflammatory activity in LPS stimulated RAW264.7 cells.

Table 4
Effect of the selected compounds against RAW264.7 cells viability.

Compound	IC$_{50}$ (μM)
4b	241.30 ± 69.20
6a	175.20 ± 24.70
6b	188.90 ± 26.00
7d	101.60 ± 16.60
8b	154.60 ± 24.20

Data is displayed as mean ± SD.

2.2.4.2. The effect of the selected compounds on the levels IL-6 and CRP in LPS-induced RAW264.7 macrophages. In response to LPS stimulation, the macrophages produce excess inflammatory mediators and cytokines like TNF-α and IL-6 [69]. In our study, the changes of the levels of IL-6 and CRP post LPS stimulation of RAW264.7 cells were first evaluated on the gene expression levels. We found that all the test compounds exerted significant anti-inflammatory effects (p < 0.001) as designated by the decreased expression levels of *CRP* and *IL-6 mRNA*. Compounds **6a** and **8b** showed the highest anti-inflammatory activity as shown by the downregulation of the *CRP* (fold change; 0.207 ± 0.021 and 0.211 ± 0.015, respectively) and *IL-6* gene expression (fold change; 0.131 ± 0.010 and 0.171 ± 0.007, respectively) compared to the mRNA levels of the LPS control group, Fig. 6. Moreover, validation of the anti-inflammatory activity on the protein level was done and the results showed that all compounds were able to significantly decrease the release of CRP and IL-6 in LPS stimulated macrophages (p < 0.001) as shown in Fig. 7. Compounds **6a** and **8b** were noted to reveal a similar pattern of activity as they reduced the release of CRP by about 75.5% and 82.6, respectively combined with the decrease in IL-6 levels by about 85.9% and 80.2%, respectively.

2.2.5. Antioxidant activity

DPPH method was utilized to test the *in vitro* antioxidant activity of the active compounds i.e., **4b, 6a, 6b, 7d,** and **8b** using Trolox as a standard. The results are shown in Table 5. **and** Fig. 8, which revealed that compounds **4b** and **8b** have the highest radical scavenging activity.

2.3. Molecular docking of the test compounds on DPP-4 enzyme

The binding modes of the most active compounds (**4b, 4c, 6a, 6b, 7d,** and **8b**) into human DPP-4 binding site were computed. The docking studies were performed against human DPP-4 active site (**PDB ID:2RGU**) [70] using **MOE 2014.09** [71]. Based on the literature, the most important residues that are responsible for DPP-4 inhibition are hydrophobic S1 pocket residues which include Tyr 631, Val 656, Trp 659, Tyr 662, Tyr 666, and Val 711, catalytic triad residues Ser 630, Asp 708, and His 740, *N*-terminal recognition region residues Glu 205, and Glu 206, and hydrophobic S2 pocket residues Arg 125, Phe 357, Arg 358, Tyr 547, Pro 550, and Asn 710 [72–75]. The co-crystallized ligand, linagliptin (pyrimidinone gliptin), can bind to the S1′ and/or S2′ subsites in addition to the S1 and S2 subsites [23,72,76].

To validate the docking protocol, the co-crystalized ligand was re-docked, and the obtained root mean square deviation (RMSD) value between the original ligand and the re-docked pose was <1°A, which indicates the reliability of the docking. The docking results of the newly
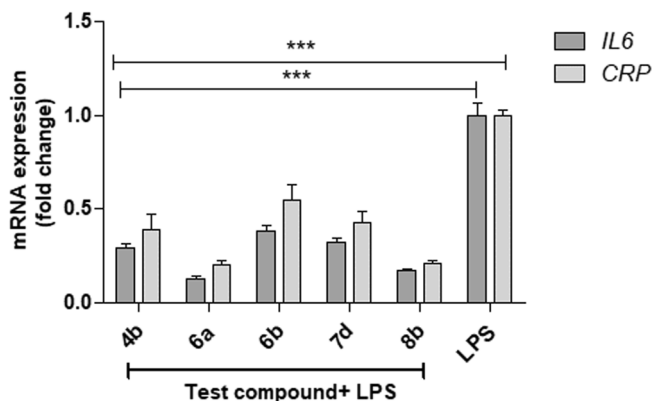

Fig. 6. The effect of selected compounds on *IL-6* **and** *CRP mRNA* **in LPS-stimulated RAW 264.7 macrophages**. Cells were treated with LPS (1 μg/mL). mRNA expression data are presented as mean ± SD fold changes of three assays referenced to *Actb*. ***: Significant (p < 0.001) compared to the mRNA levels of the LPS control group. *Actb*: β-actin; the housekeeping gene.
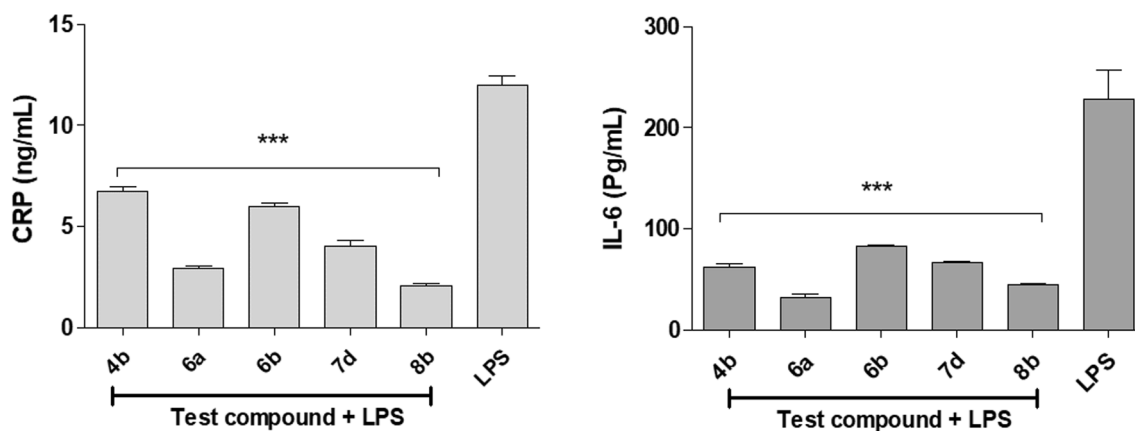
Fig. 7. Effect of the selected compounds on the release of CRP and IL-6 by LPS (1 µg/mL) stimulated RAW264.7 macrophages. Data are presented as mean ± SD of three assays. ***: Significant ($p < 0.001$) compared to LPS.

Table 5
Antioxidant activity of the most active compounds using the DPPH scavenging method.

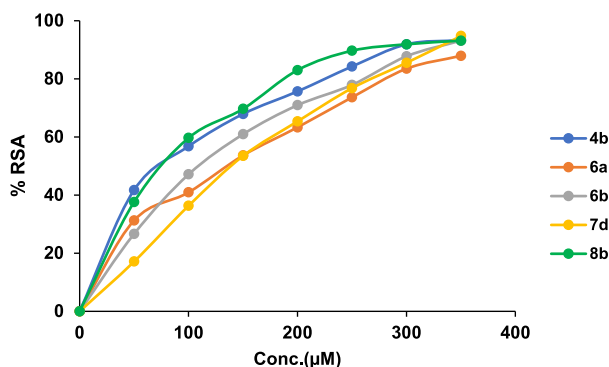| Compound	IC50 (µM)
4b	65.93 ± 3.4
6a	138.71 ± 7.1
6b	123.02 ± 6.3
7d	155.14 ± 7.9
8b	60.79 ± 3.1
Trolox	55.18 ± 2.8

Data is displayed as mean ± SD.

Fig. 8. % Radical scavenging activity of the test compounds in DPPH assay.

synthesized compounds were compared to the reported ligand. The results of energy binding scores and binding interactions are depicted in Table 6 and Figs. 9 and 10.

The co-crystalized ligand (Linagliptin) docking results exhibited a docking score −6.0368 Kcal/mol, it formed three hydrogen bonds with Glu205, Glu 206, and Tyr631 at distances 2.85, 2.82, and 3.29 A°, respectively, and one H-π interaction between Tyr547 and its imidazole moiety at a distance of 3.78 A°, in addition to one π-π interaction between Trp629 and its phenyl group (3.85 A°).

Our compounds **(4b,c, 6a,b, 7d, & 8b)** share with linagliptin the binding to two or three residues. Hydrazines **6a**, and hydrazones **8b**, both share linagliptin in binding with three residues through formation of four bindings. Like linagliptin, compound **6a** binds to residues Glu205, Tyr547, and Trp629, where it forms one hydrogen bond with Glu205, two π-H interactions with Tyr547 phenyl and one H-π interaction of Trp629 with its phenyl moiety, in addition to other two hydrogen bonds with Arg125, and Asn710. While **8b** shares linagliptin with binding with residues Tyr631, Tyr547, and Trp629. It exhibited two H-π

interactions with Tyr631 and Trp629, in addition to other two bindings with Tyr547. Also, it displayed a cation-π interaction with Lys554 and one hydrogen bond with Asn710. Moreover, they both have the best binding scores (−6.9885 and −6.7936 Kcal/mol, respectively). These results are consistent with the biological results and can explain the highest inhibitory activity of compounds **6a** and **8b** against DPP-4. On the other hand, thiazolopyrimidines **4b** and **4c**, pyrimidine derivative **6b** and triazolopyrimidine **7d** share linagliptin with binding with only two residues with docking scores −6.1787, −5.4205, −6.2857, and −5.6598 Kcal/mol, respectively. Compound **4b** exhibited three hydrogen bonds with the key residues Glu206, Tyr547, and Arg125. Compound **4c** displayed one π-H interaction with Tyr547 and one H-π interaction between Trp629 and its tolyl moiety. Pyrimidine derivative **6b** presented three hydrogen bonds with Glu206, Arg125, and Asn710, in addition to one H-π interaction between Trp629 and its tolyl group. Finally, triazolopyrimidine **7d** exhibited three hydrogen bonds with Glu205, Tyr631, and Asn710.

On exploring the structure activity relationship (SAR), from the biological screening results of the test compounds, we found that compounds **6a** and **7d** showed the highest DPP-4 inhibitory activity compared to linagliptin, in the *in vitro DPP-4* inhibition assay, as well as in the *in vivo* study that was carried on type 2 diabetic rats. Furthermore, investigation of the antidiabetic effect of our synthesized compounds in type 2 diabetic rats, revealed that **6b** and **4b** displayed better glycemic control than linagliptin. Finally, **4b** and **8b** demonstrated potent radical scavenging activity in DPPH assay, while **6a** and **8b** showed the highest anti-inflammatory activity in LPS-induced RAW264.7 macrophages as shown by the down-regulation of the CRP and IL-6 gene expression and protein levels as revealed in Fig. 11, which indicates the full SAR of our tested compounds.

3. Conclusion

A novel series of pyrimidinone and thio-pyrimidinone derivatives were synthesized, and evaluated for their *in vivo* antihyperglycemic, and *in vitro* DPP-4 inhibitory activity. The most active compounds i.e., **4b, 6a,b, 7d, & 8b** were tested for their *in vivo* antidiabetic effect and plasma DPP-4 inhibitory activity as well as, their antioxidant and anti-inflammatory activities. All the *in vitro* results are compatible with the docking results. Summarizing the results indicated that compound **8b** was one of the most promising bioactive hydrazones, offered the highest activity as DPP-4I, with promising anti-inflammatory, antioxidant effects and may be able to significantly mitigate COVID-19 in type 2 diabetic patients. The results of this research may be a flashlight in the dark to discover a valuable therapeutic means for type 2 diabetic patients coupled with anti-inflammatory activities and a protecting effect against COVID-19 infection outcomes.

Table 6
Results of molecular docking of the most active compounds* versus DPP-4 (PDB ID: 2RGU).

Compound	(S) Kcal/mol	E score1 Kcal/mol	E score 2 Kcal/mol	Binding interaction (Receptor-Ligand)
4b	−6.1787	−10.9107	−6.1787	Glu206-(Thiazole) (H-b, 4.10 A°), Tyr547-(C=O*-Pyrimidine) (H-b, 2.86 A°), Arg125-(C=S) (H-b, 3.31 A°).
4c	−5.4205	−11.5807	−5.4205	Tyr547-(*NH-C=O) (π-H, 3.94 A°), Trp629-(Tolyl) (H-π, 4.24 A°).
6a	−6.9885	−11.3901	−6.9885	Glu205-(*NH-NH₂) (H-b, 3.40 A°), Tyr547-(*NH-C=S) (π-H, 4.26 A°), Tyr547-(Phenyl) (π-H, 4.13 A°), Trp629-(Phenyl) (H-π, 3.85 A°), Arg125-(C=S) (H-b, 4.42 A°), Asn710-(C=O) (H-b, 3.26 A°).
6b	−6.2857	−11.1729	−6.2857	Glu206-(*NH-NH₂) (H-b, 3.03 A°), Trp629-(Tolyl) (H-π, 4.15 A°), Arg125-(S=O) (H-b, 3.04 A°), Asn710-(C=O) (H-b, 2.98 A°).
7d	−5.6598	−10.6269	−5.6598	Glu205-(NH-Phenyl) (H-b, 3.08 A°), Tyr631-(C=O) (H-b, 3.07 A°), Asn710-(NH-C=O*) (H-b, 3.40 A°).
8b	−6.7936	−11.2189	−6.7936	Tyr631-(Pyrimidine) (H-π, 4.70 A°), Tyr547-(C=S) (H-b, 3.72 A°), Tyr547-(*NH—N=CH—) (π-H, 3.80A°), Trp629-(Phenyl) (H-π, 4.05A°), Lys554-(Phenyl) (cation- π, 4.59 A°), Asn710-(S=O) (H-b, 3.09 A°).
Linagliptin	−6.0368	−11.3452	−6.0368	Glu205-(NH₃⁺) (H-b, 2.85 A°), Glu206-(NH₃⁺) (H-b, 2.82 A°), Tyr631-(C=O) (H-b, 3.29 A°), Tyr547-(Imidazole) (H-π, 3.78 A°), Trp629-(Phenyl) (π-π, 3.85 A°).

The most active compounds* (4b, 4c, 6a, 6b, 7d, and 8b)

4. Experimental

4.1. Chemistry

4.1.1. Material and methods

All commercial chemicals used as starting materials and reagents in this study were purchased from Merck (Darmstadt, Germany) and were of reagent grade. All melting points were uncorrected and measured using Electro-thermal IA 9100 apparatus (Shimadzu, Japan); IR spectra were recorded as potassium bromide pellets on a Perkin-Elmer 1650 spectrophotometer (USA), Faculty of Science, Cairo University, Cairo, Egypt. ^{1}H NMR spectra were determined on a Varian Mercury (300 MHz) spectrometer (Varian UK) and chemical shifts were expressed as ppm against TMS as internal reference (The Main Chemical Warfare Laboratories, Almaza, Cairo, Egypt). Mass spectra were recorded on 70 eV (EI Ms-QP 1000 EX, Shimadzu, Japan), Faculty of Science, Cairo University, Cairo, Egypt. Microanalyses were operated using Vario, Elmentar apparatus (Shimadzu, Japan), Organic Microanalysis Unit, Faculty of Science, Cairo University, Cairo, Egypt. Column Chromatography was performed on (Merck) Silica gel 60 (particle size 0.06–0.20 mm). All the listed compounds are new except compounds **1,2** were previously reported [39,77,78].

4.1.2. General procedure for the synthesis of compounds 3a-d

A mixture of sulfonyl chloride 2 (1.13 g, 0.005 mol) and the appropriate substituted urea or thiourea (0.005 mol) in sodium ethoxide/ethanol mixture (25 mL) was refluxed for 15–20 h, then cooled, filtered off, dried under suction, and recrystallized from DMF/water to give compounds **3a-d**.

1-[(4-Oxo-2-thioxo-1H-pyrimidin-5-yl)sulfonyl]-3-phenyl-thiourea (3a): Yield: 62%; m.p.: 278–280 °C; IR (KBr) υ (cm^{-1}): 3360–3012 (NH, broad), 1682 (C=O), 1381,1168 (SO₂); MS (EI) *m/z*: 342 (M⁺, 60.1%); ^{1}H NMR (DMSO-d_6, 300 MHz) δ (ppm): 7.34–7.74 (m, 5H, Ar-H), 8.21 (s, 1H, pyrimidine), 11.14, 11.30, 12.05, 12.71 (s, 4NH, D₂O exchangeable); ^{13}C NMR (DMSO, 75 MHz) δ (ppm): 99.13, 102.11, 118.13, 122.43, 125.53, 143.42 (SP² carbon atoms), 152.3 (C=O), 162.27, 169.1 (C=S); Anal. Calcd. for C₁₁H₁₀N₄O₃S₃ (341.99): C, 38.60; H, 2.92; N, 16.37%. Found: C, 38.79; H, 3.06; N, 16.14%.

3-(4-Methylphenyl)-1-[(4-oxo-2-thioxo-1H-pyrimidin-5-yl)sulfonyl]-thiourea (3b): Yield: 67%; m.p.: 207–209 °C; IR (KBr) υ (cm^{-1}): 3414–3088 (NH, broad), 1680 (C=O), 1396,1170 (SO₂); MS (EI) *m/z*: 356 (M⁺, 28.21%); ^{1}H NMR (DMSO-d_6, 300 MHz) δ (ppm): 3.71 (s, 3H, CH₃), 7.22–7.75 (m, 4H, Ar-H), 8.50 (s, 1H, pyrimidine), 11.14, 11.31, 12.57, 12.64 (s, 4NH, D₂O exchangeable); Anal. Calcd. for C₁₂H₁₂N₄O₃S₃ (356.07): C, 40.45; H, 3.37; N, 15.73%. Found: C, 40.27; H, 3.14; N, 15.99%.

1-[(4-Oxo-2-thioxo-1H-pyrimidin-5-yl)sulfonyl]-3-phenyl-urea (3c): Yield: 79%; m.p.: >300 °C; IR (KBr) υ (cm^{-1}): 3357–3010 (NH, broad), 1688, 1661 (2C=O), 1406,1200 (SO₂); MS (EI) *m/z*: 326 (M⁺, 15.19%); ^{1}H NMR (DMSO-d_6, 300 MHz) δ (ppm): 6.68–7.07 (m, 5H, Ar-H), 8.23 (s, 1H, pyrimidine), 10.02, 10.34, 11.34, 11.76 (s, 4NH, D₂O exchangeable); Anal. Calcd. for C₁₁H₁₀N₄O₄S₂ (326.14): C, 40.49; H, 3.07; N, 17.18%. Found: C, 40.77; H, 3.31; N, 17.23%.

3-(4-Methylphenyl)-1-[(4-oxo-2-thioxo-1H-pyrimidin-5-yl)sulfonyl]-urea (3d): Yield: 81%; m.p.: 222–224 °C; IR (KBr) υ (cm^{-1}): 3366–3028 (NH, broad), 1687, 1659 (2C=O), 1390,1177 (SO₂); MS (EI) *m/z*: 340 (M⁺, 46.92%); ^{1}H NMR (DMSO-d_6, 300 MHz) δ (ppm): 2.42 (s, 3H, CH₃), 6.98–7.43 (m, 4H, Ar-H), 8.24 (s, 1H, pyrimidine), 10.17, 10.24, 10.81, 11.25 (s, 4NH, D₂O exchangeable); Anal. Calcd. for C₁₂H₁₂N₄O₄S₂ (340.29): C, 42.35; H, 3.53; N, 16.47%. Found: C, 42.08; H, 3.44; N, 16.31%.

4.1.3. General procedure for the synthesis of compounds 4a-d

To an ice-cold solution of **3a–d** (0.01 mol) in 40 mL DMF, triethyl amine (0.03 mol) and chloroacetyl chloride (0.03 mol) were added successively. The reaction mixture was heated in a water bath at 70 °C for 6 h, cooled, poured into ice / cold water and extracted with methylene chloride (3 × 30 mL). The organic layer was dried on anhydrous sodium sulphate, filtered off and the filtrate was evaporated to dryness. The residue was washed with 10% sodium carbonate solution and the un-dissolved solid was filtered off, dried, and recrystallized from DMF/water to give compounds **4a–d**.

1-[(2,5-Dioxo-8,8a-dihydro-3H-thiazolo[3,2-a]pyrimidin-6-yl)sulfonyl]-3-phenyl-thiourea (4a): Yield: 64%; m.p.: 216–218 °C; IR (KBr) υ (cm^{-1}): 3409–3085 (NH, broad), 1687, 1662 (2C=O),
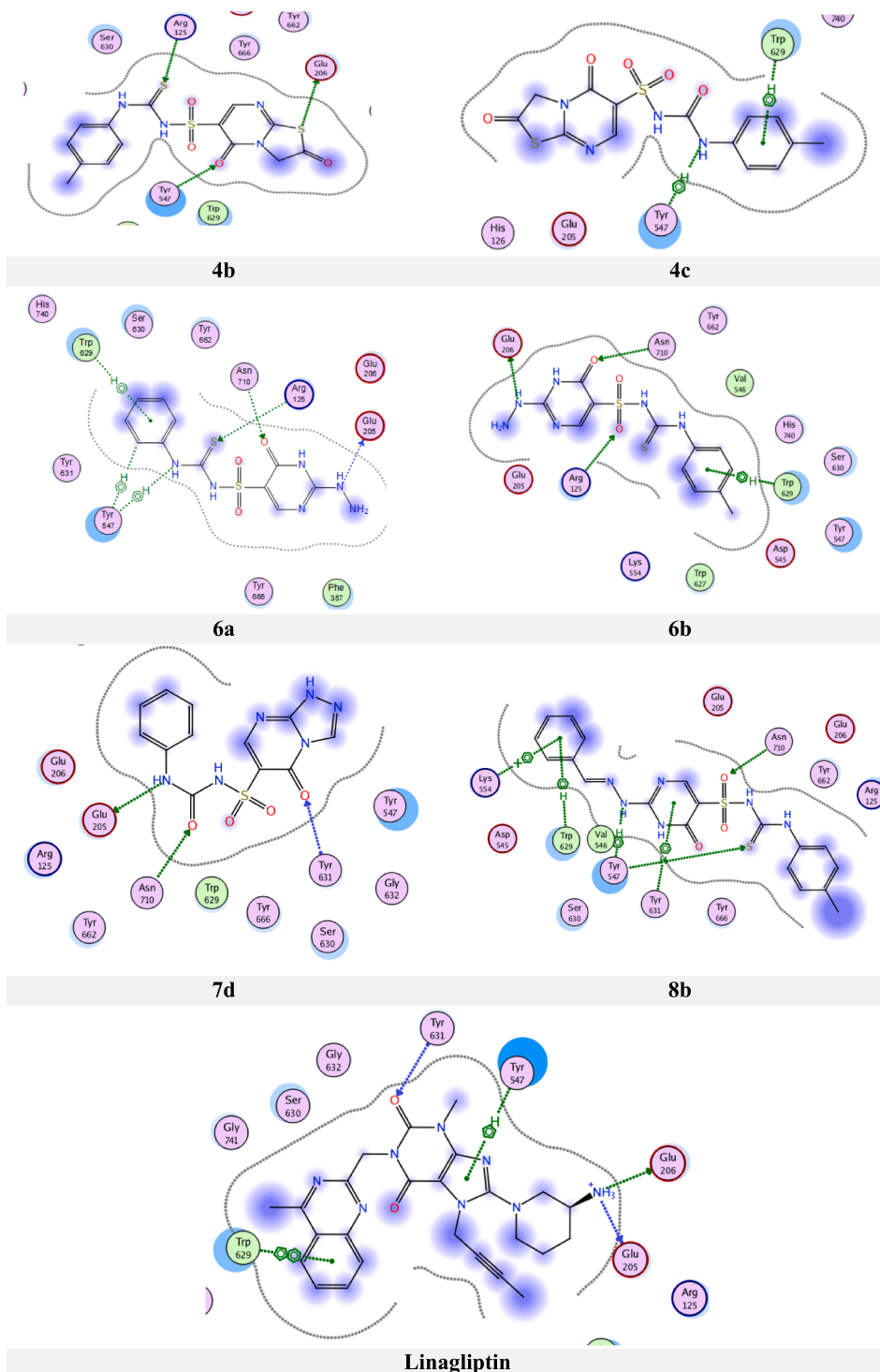
Fig. 9. 2D binding modes of compounds (4b, 4c, 6a, 6b, 7d, 8b) and Linagliptin with DPP-4 active site.

1385,1178 (SO$_2$); MS (EI) *m/z*: 384 (M$^+$, 37.6%); ^{1}H NMR (DMSO-*d$_6$*, 300 MHz) δ (ppm): 3.41 (s, 2H, CH$_2$), 4.68 (s,1H, CH-fusion), 7.12–7.83 (m, 5H, Ar-H), 8.16 (s, 1H, pyrimidine), 11.30, 11.41, 11.65 (s, 3NH, D$_2$O exchangeable); Anal. Calcd. for C$_{13}$H$_{12}$N$_4$O$_4$S$_3$ (384.02): C, 40.63; H, 3.13; N, 14.58%. Found: C, 40.88; H, 3.02; N, 14.23%.

3-(4-Methylphenyl)-1-[(2,5-dioxo-8,8a-dihydro-3H-thiazolo[3,2-a]pyrimidin-6-yl)sulfonyl]-thiourea (4b): Yield: 75%; m.p.: 242–244 °C; IR (KBr) υ (cm^{-1}): 3379–3102 (NH, broad), 1693, 1667 (2C=O), 1405,1199 (SO$_2$); MS (EI) *m/z*: 398 (M$^+$, 90.2%); ^{1}H NMR (DMSO-*d$_6$*, 300 MHz) δ (ppm): 2.32 (s, 3H, CH$_3$), 3.58 (s, 2H, CH$_2$), 3.91

(s,1H, CH-fusion), 7.32–7.42 (m, 4H, Ar-H), 8.16 (s, 1H, pyrimidine), 11.14, 11.29, 12.70 (s, 3NH, D$_2$O exchangeable); ^{13}C NMR (DMSO, 75 MHz) δ (ppm): 35.71 (CH$_3$), 39.24, 40.49 (C—N), 99.82, 104.07, 116.98, 122.41, 133.12, 145.25 (SP^2 carbon atoms), 151.54, 162.75 (C=O), 165.57 (C=S); Anal. Calcd. for C$_{14}$H$_{14}$N$_4$O$_4$S$_3$ (398.02): C, 42.21; H, 3.52; N, 14.07%. Found: C, 42.34; H, 3.41; N, 14.31%.

1-[(2,5-Dioxo-8,8a-dihydro-3H-thiazolo[3,2-a]pyrimidin-6-yl)sulfonyl]-3-phenyl-urea(4c): Yield: 71%; m.p.: 190–192 °C; IR (KBr) υ (cm^{-1}): 3410–3103 (NH, broad), 1702, 1681, 1668 (3C=O), 1373,1169 (SO$_2$); MS (EI) *m/z*: 368 (M$^+$, 8.64%); ^{1}H NMR (DMSO-*d$_6$*, 300 MHz) δ
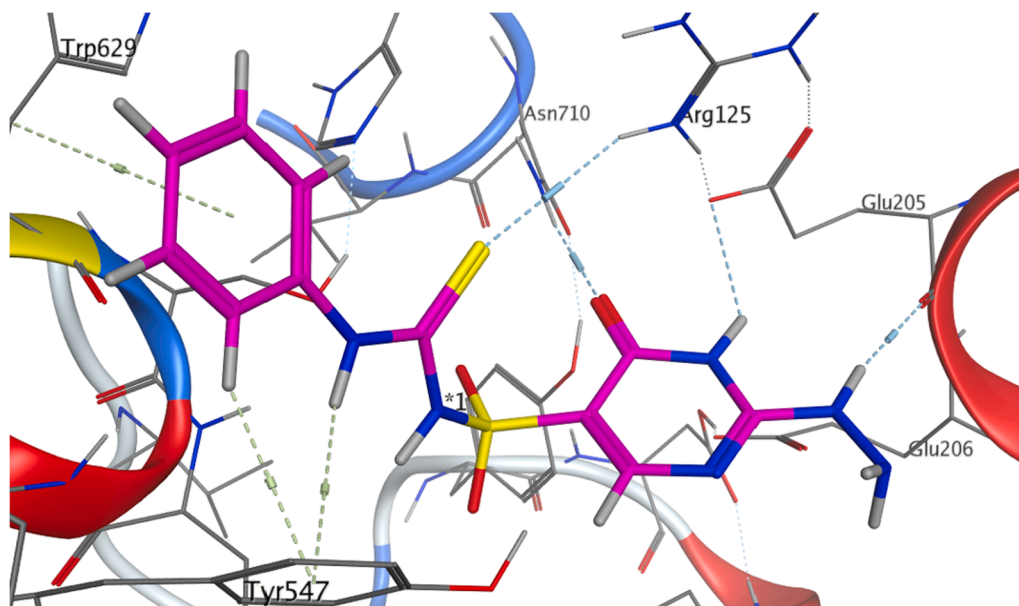
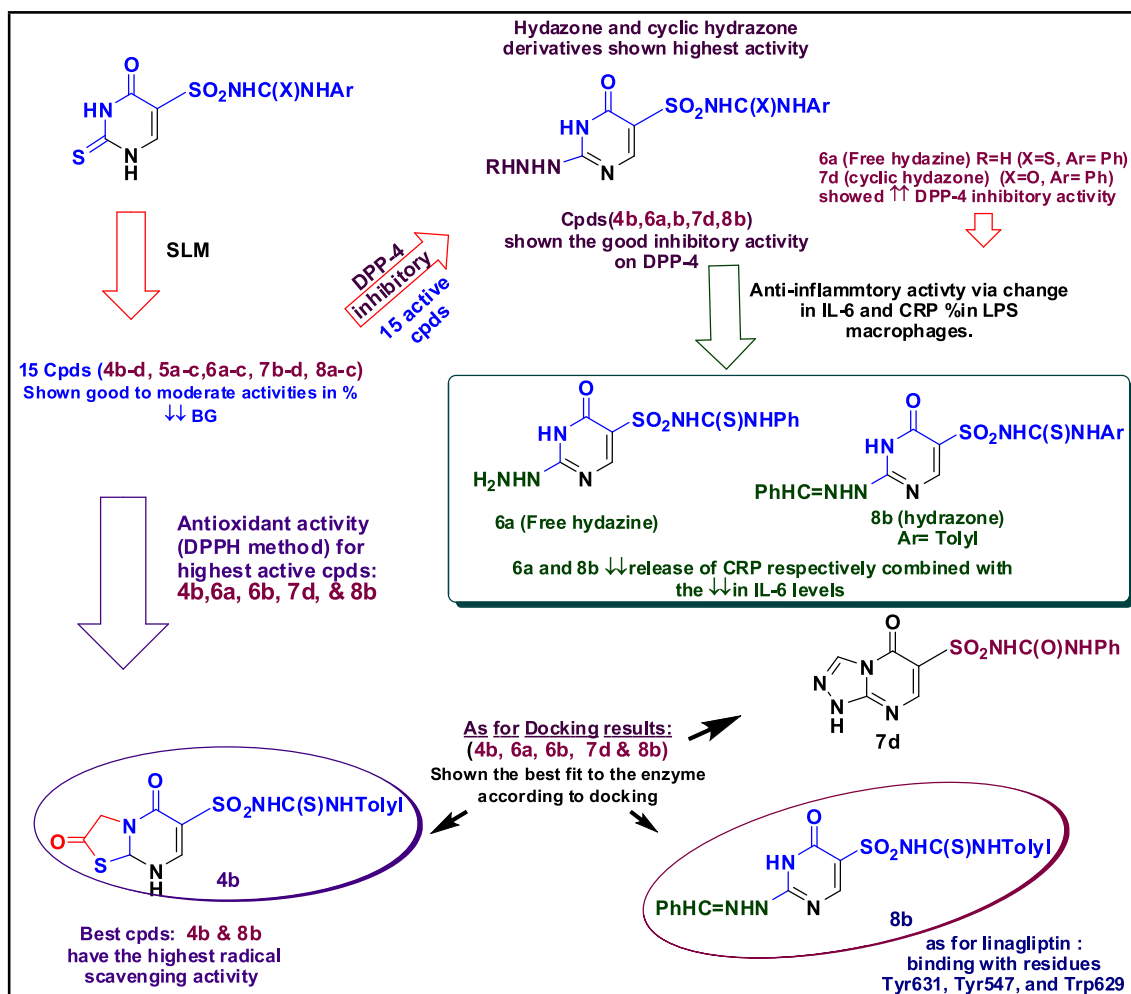**Fig. 10.** 3D binding mode of compound 6a with DPP-4 active site.

Fig. 11. SAR for the uppermost active compounds.

(ppm): 3.39 (s, 2H, CH$_2$), 3.83 (s,1H, CH-fusion), 7.31–7.85 (m, 5H, Ar-H), 8.19 (s, 1H, pyrimidine), 11.14, 11.31, 12.02 (s, 3NH, D$_2$O exchangeable); ^{13}C NMR (DMSO, 75 MHz) δ (ppm): 38.17 (CH$_3$), 39.27, 40.52 (C—N), 102.33, 105.74, 108.34, 118.11, 131.25, 142.54 (SP^2 carbon atoms), 161.50, 170.02, 176.51 (C=O); Anal. Calcd. for C$_{13}$H$_{12}$N$_4$O$_5$S$_2$ (368.02): C, 42.39; H, 3.26; N, 15.22%. Found: C, 42.68; H, 3.07; N, 14.99%.

3-(4-Methylphenyl)-1-[[2,5-dioxo-8,8a-dihydro-3H-thiazolo[3,2-a]pyrimidin-6-yl)sulfonyl]-urea (4d): Yield: 80%; m.p.: 239–241 °C; IR (KBr) υ (cm^{-1}): 3382–3148 (NH, broad), 1703, 1683, 1655 (3C=O), 1410,1200 (SO$_2$); MS (EI) *m/z*: 382 (M$^+$, 44.14%); ^{1}H NMR (DMSO-*d$_6$*, 300 MHz) δ (ppm): 2.71 (s, 3H, CH$_3$), 5.80 (s, 2H, CH$_2$), 5.82 (s,1H, CH-fusion), 7.20–7.61 (m, 4H, Ar-H), 8.13 (s, 1H, pyrimidine), 11.03, 12.25, 12.42 (s, 3NH, D$_2$O exchangeable); ^{13}C NMR (DMSO, 75 MHz) δ (ppm): 35.22 (CH$_3$), 39.25, 40.50 (C—N), 97.66, 104.00, 110.10, 119.25, 133.76, 145.25 (SP^2 carbon atoms), 151.54, 158.22, 162.75 (C=O); Anal. Calcd. for C$_{14}$H$_{14}$N$_4$O$_5$S$_2$ (382.04): C, 43.98; H, 3.66; N, 14.66%. Found: C, 44.13; H, 3.45; N, 14.49%.

4.1.4. General procedure for the synthesis of compounds 5a-d

To a solution of monochloroacetic acid (0.03 mol) and sodium hydroxide (0.03 mol) in 5 mL water, a solution of **3a-d** (0.03 mol) and sodium hydroxide (0.03 mol) in 10 mL water was added. The reaction mixture was stirred at ambient temperature for 4 h and rendered acidic with hydrochloric acid (6 N). The separated solid was filtered off, washed with water and recrystallized from methanol to obtain compounds **5a-d**.

2-[[6-Oxo-5-(phenylcarbamothioylsulfamoyl)-1H-pyrimidin-2-yl]sulfanyl]acetic acid (5a).

Yield: 62%; m.p.: >300 °C; IR (KBr) υ (cm^{-1}): 3428–3074 (OH, NH, broad), 1756, 1681 (2C=O), 1401,1183 (SO$_2$); MS (EI) *m/z*: 400 (M$^+$, 17.21%); ^{1}H NMR (DMSO-*d$_6$*, 300 MHz) δ (ppm): 5.39 (s, 2H, CH$_2$), 6.92–7.72 (m, 5H, Ar-H), 8.61 (s, 1H, pyrimidine), 10.87, 11.19, 11.27, 11.65 (s, 3NH, OH, D$_2$O exchangeable); Anal. Calcd. for C$_{13}$H$_{12}$N$_4$O$_5$S$_3$ (399.99): C, 39.00; H, 3.00; N, 14.00%. Found: C, 39.17; H, 2.82; N, 14.08%.

2-[[5-(4-Methylphenylcarbamothioylsulfamoyl)-6-oxo-1H-pyrimidin-2-yl]sulfanyl]acetic acid (5b).

Yield: 67%; m.p.: 265–267 °C; IR (KBr) υ (cm^{-1}): 3476–3041 (OH, NH, broad), 1760, 1683 (2C=O), 1403,1172 (SO$_2$); MS (EI) *m/z*: 414 (M$^+$, 41.2%); ^{1}H NMR (DMSO-*d$_6$*, 300 MHz) δ (ppm): 2.81 (s, 1H, CH$_3$), 5.48 (s, 2H, CH$_2$), 6.983–7.73 (m, 4H, Ar-H), 8.12 (s, 1H, pyrimidine), 9.01, 11.39, 120.31, 13.15 (s, 3NH, OH, D$_2$O exchangeable); Anal. Calcd. for C$_{14}$H$_{14}$N$_4$O$_5$S$_3$ (414.01): C, 40.58; H, 3.38; N, 13.53%. Found: C, 40.22; H, 3.70; N, 13.41%.

2-[[6-Oxo-5-(phenylcarbamoylsulfamoyl)-1H-pyrimidin-2-yl]sulfanyl]acetic acid (5c).

Yield: 75%; m.p.: 240–242 °C; IR (KBr) υ (cm^{-1}): 3437–3104 (OH, NH, broad), 1763, 1687, 1664 (3C=O), 1388,1169 (SO$_2$); MS (EI) *m/z*: 384 (M$^+$, 18.61%); ^{1}H NMR (DMSO-*d$_6$*, 300 MHz) δ (ppm): 5.67 (s, 2H, CH$_2$), 6.79–7.88 (m, 5H, Ar-H), 8.31 (s, 1H, pyrimidine), 9.86, 11.99, 12.23, 12.28 (s, 3NH, OH, D$_2$O exchangeable); ^{13}C NMR (DMSO, 75 MHz) δ (ppm): 18.52 (CH$_2$-S), 104.13, 110.24, 118.74, 135.27, 139.16, 148.25 (SP^2 carbon atoms), 153.61, 161.49, 176.30 (C=O); Anal. Calcd. for C$_{13}$H$_{12}$N$_4$O$_6$S$_2$ (384.02): C, 40.63; H, 3.13; N, 14.58%. Found: C, 40.72; H, 3.08; N, 14.75%.

2-[[5-(4-Methylphenylcarbamoylsulfamoyl)-6-oxo-1H-pyrimidin-2-yl]sulfanyl]acetic acid (5d).

Yield: 77%; m.p.: 262–264 °C; IR (KBr) υ (cm^{-1}): 3460–3090 (OH, NH, broad), 1759, 1680, 1661 (3C=O), 1409,1199 (SO$_2$); MS (EI) *m/z*: 398 (M$^+$, 27.3%); ^{1}H NMR (DMSO-*d$_6$*, 300 MHz) δ (ppm): 2.51 (s, 1H, CH$_3$), 5.82 (s, 2H, CH$_2$), 7.00–7.57 (m, 4H, Ar-H), 8.13 (s, 1H, pyrimidine), 10.81, 11.02, 12.25, 12.42 (s, 3NH, OH, D$_2$O exchangeable); ^{13}C NMR (DMSO, 75 MHz) δ (ppm): 24.15 (CH$_2$-S), 39.25 (CH$_3$), 105.74, 108.41, 118.33, 124.67, 127.04, 142.55 (SP^2 carbon atoms), 161.51, 169.42, 176.50 (C=O); Anal. Calcd. for C$_{14}$H$_{14}$N$_4$O$_6$S$_2$ (398.04): C,

42.21; H, 3.52; N, 14.07%. Found: C, 42.29; H, 3.41; N, 13.89%.

4.1.5. General procedure for the synthesis of compounds 6a-d

A mixture of **3a-d** (0.005 mol) and hydrazine hydrate 99% (0.005 mol) in 30 mL methanol was refluxed for 30 h, then cooled and poured into ice/water. The produced solid was filtered off, dried, and recrystallized from methanol to give compounds **6a-d**.

1-[(2-Hydrazino-6-oxo-1H-pyrimidin-5-yl)sulfonyl]-3-phenyl-thiourea (6a): Yield: 78%; m.p.: 170–172 °C; IR (KBr) υ (cm^{-1}): 3478–3090 (NH$_2$, NH, broad), 1685 (C=O), 1410,1168 (SO$_2$); MS (EI) *m/z*: 340 (M$^+$, 24.41%); ^{1}H NMR (DMSO-*d$_6$*, 300 MHz) δ (ppm): 5.38 (s, 2H, NH$_2$-Hydrazine, D$_2$O exchangeable), 6.95–7.30 (m, 5H, Ar-H), 8.22 (s, 1H, pyrimidine), 9.90, 10.72, 10.90, 11.03 (s, 4H-4*NH, D$_2$O exchangeable); Anal. Calcd. for C$_{11}$H$_{12}$N$_6$O$_3$S$_2$ (340.04): C, 38.82; H, 3.53; N, 24.71%. Found: C, 39.06; H, 3.80; N, 24.66%.

1-[(2-Hydrazino-6-oxo-1H-pyrimidin-5-yl)sulfonyl]-3-(4-methyl-phenyl)-thiourea (6b): Yield: 82%; m.p.: 189–191 °C; IR (KBr) υ (cm^{-1}): 3428–3077 (NH$_2$, NH, broad), 1673 (C=O), 1397,1171 (SO$_2$); MS (EI) *m/z*: 354 (M$^+$, 18.97%); ^{1}H NMR (DMSO-*d$_6$*, 300 MHz) δ (ppm): 2.41 (s, 3H, CH$_3$), 5.17 (s, 2H, NH$_2$-Hydrazine, D$_2$O exchangeable), 6.98–7.25 (m, 4H, Ar-H), 8.31 (s, 1H, pyrimidine), 9.95, 10.65, 10.87, 11.16 (s, 4H-4*NH, D$_2$O exchangeable); ^{13}C NMR (DMSO, 75 MHz) δ (ppm): 39.26 (CH$_3$), 104.12, 105.41, 109.48, 119.77, 124.23, 127.24, 142.55 (SP^2 carbon atoms), 161.51 (C=O), 176.29 (C=S); Anal. Calcd. for C$_{12}$H$_{14}$N$_6$O$_3$S$_2$ (354.06): C, 40.68; H, 3.95; N, 23.73%. Found: C, 40.61; H, 3.83; N, 23.94%.

1-[(2-Hydrazino-6-oxo-1H-pyrimidin-5-yl)sulfonyl]-3-phenyl-urea (6c): Yield: 69%; m.p.: 200–202 °C; IR (KBr) υ (cm^{-1}): 3493–3104 (NH$_2$, NH, broad), 1671 (C=O), 1394,1170 (SO$_2$); MS (EI) *m/z*: 324 (M$^+$, 18.3%); ^{1}H NMR (DMSO-*d$_6$*, 300 MHz) δ (ppm): 5.40 (s, 2H, NH$_2$-Hydrazine, D$_2$O exchangeable), 6.98–7.24 (m, 5H, Ar-H), 8.37 (s, 1H, pyrimidine), 10.08, 10.82, 11.17, 11.68 (s, 4H-4*NH, D$_2$O exchangeable); Anal. Calcd. for C$_{11}$H$_{12}$N$_6$O$_4$S (324.06): C, 40.74; H, 3.70; N, 25.93%. Found: C, 40.63; H, 3.81; N, 25.62%.

1-[(2-Hydrazino-6-oxo-1H-pyrimidin-5-yl)sulfonyl]-3-(4-methyl-phenyl)-urea (6d): Yield: 73%; m.p.: 165–167 °C; IR (KBr) υ (cm^{-1}): 3480–3117 (NH$_2$, NH, broad), 1685 (C=O), 1391,1188 (SO$_2$); MS (EI) *m/z*: 338 (M$^+$, 8.07%); ^{1}H NMR (DMSO-*d$_6$*, 300 MHz) δ (ppm): 2.34 (s, 3H, CH$_3$), 5.51 (s, 2H, NH$_2$-Hydrazine, D$_2$O exchangeable), 7.09–7.45 (m, 4H, Ar-H), 8.33 (s, 1H, pyrimidine), 10.44, 10.82, 11.19, 11.49 (s, 4H-4*NH, D$_2$O exchangeable); ^{13}C NMR (DMSO, 75 MHz) δ (ppm): 39.13 (CH$_3$), 94.94, 104.33, 106.56, 109.22, 118.12, 123.18, 142.66 (SP^2 carbon atoms), 151.35, 165.87 (C=O); Anal. Calcd. for C$_{12}$H$_{14}$N$_6$O$_4$S (338.08): C, 42.60; H, 4.14; N, 24.85%. Found: C, 42.67; H, 4.29; N, 24.61%.

4.1.6. General procedure for the synthesis of compounds 7a-d

A mixture of hydrazino compounds **6a-d** (0.001 mol) and 30 mL formic acid was refluxed for 8 h, then cooled and poured into ice/water and the precipitate was filtered off, dried, and recrystallized from methanol to give compounds **7a-d**.

1-[(5-oxo-1H-[1,2,4]triazolo[4,3-a]pyrimidin-6-yl)sulfonyl]-3-phenyl-thiourea (7a):

Yield: 67 %; m.p.: 186–188 °C; IR (KBr) υ (cm^{-1}): 3359–3125 (NH, broad), 1685 (C=O), 1383,1168 (SO$_2$); MS (EI) *m/z*: 350 (M$^+$, 50.36%); ^{1}H NMR (DMSO-*d$_6$*, 300 MHz) δ (ppm): 7.28–7.85 (m, 7H, Ar-H), 10.23, 11.16, 11.31 (s, 3NH, D$_2$O exchangeable);); ^{13}C NMR (DMSO, 75 MHz) δ (ppm): 94.94, 104.33, 106.56, 109.22, 118.12, 123.18, 142.66 (SP^2 carbon atoms), 151.54 (C=O), 162.76 (C=S); Anal. Calcd. for C$_{12}$H$_{10}$N$_6$O$_3$S$_2$ (350.03): C, 41.14; H, 2.86; N, 24.00%. Found: C, 40.98; H, 2.82; N, 24.12%.

1-[(5-oxo-1H-[1,2,4]triazolo[4,3-a]pyrimidin-6-yl)sulfonyl]-3-(4-methylphenyl)-thiourea (7b): Yield: 69 %; m.p.: 242–244 °C; IR (KBr) υ (cm^{-1}): 3410–3127 (NH, broad), 1694 (C=O), 1380,1173 (SO$_2$); MS (EI) *m/z*: 364 (M$^+$, 14.1%); ^{1}H NMR (DMSO-*d$_6$*, 300 MHz) δ (ppm): 2.34 (s, 3H, CH$_3$), 7.23–8.17 (m, 6H, Ar-H), 9.81, 9.96, 10.06 (s, 3NH,

D$_2$O exchangeable); ^{13}C NMR (DMSO, 75 MHz) δ (ppm): 39.28 (CH$_3$), 93.02, 105.33, 109.73, 114.18, 119.02, 123.21, 142.66, 143.35 (SP^2 carbon atoms), 161.87 (C=O), 175.45 (C=S); Anal. Calcd. for C$_{13}$H$_{12}$N$_6$O$_3$S$_2$ (364.04): C, 42.86; H, 3.30; N, 23.08%. Found: C, 42.81; H, 3.25; N, 23.23%.

1-[(5-oxo-1H-[1,2,4]triazolo[4,3-a]pyrimidin-6-yl)sulfonyl]-3-phenyl-urea (7c): Yield: 64 %; m.p.: >300 °C; IR (KBr) υ (cm^{-1}): 3322–3095 (NH, broad), 1685, 1667 (2C=O), 1371,1166 (SO$_2$); MS (EI) *m/z*: 334 (M$^+$, 9%); ^{1}H NMR (DMSO-*d$_6$*, 300 MHz) δ (ppm): 6.97–8.23 (m, 7H, Ar-H), 10.70, 11.30, 11.68 (s, 3NH, D$_2$O exchangeable); Anal. Calcd. for C$_{12}$H$_{10}$N$_6$O$_4$S (334.05): C, 43.11; H, 2.99; N, 25.15%. Found: C, 43.16; H, 2.90; N, 25.26%.

1-[(5-oxo-1H-[1,2,4]triazolo[4,3-a]pyrimidin-6-yl)sulfonyl]-3-(4-methylphenyl)-urea(7d): Yield: 61 %; m.p.: 235–237 °C; IR (KBr) υ (cm^{-1}): 3409–3127 (NH, broad), 1690, 1666 (2C=O), 1359,1168 (SO$_2$); MS (EI) *m/z*: 348 (M$^+$, 24.32%); ^{1}H NMR (DMSO-*d$_6$*, 300 MHz) δ (ppm): 2.41 (s, 3H, CH$_3$), 6.96–7.83 (m, 6H, Ar-H), 9.93, 10.30, 10.87 (s, 3NH, D$_2$O exchangeable); Anal. Calcd. for C$_{13}$H$_{12}$N$_6$O$_4$S (348.06): C, 44.83; H, 3.45; N, 24.14%. Found: C, 44.69; H, 3.34; N, 24.21%.

4.1.7. General procedure for the synthesis of compounds 8a-d

A mixture of hydrazino compounds **6a-d** (0.001 mol) and benzaldehyde (0.001 mol) in 30 mL methanol was heated under reflux, then cooled and the produced precipitate was filtered off, dried, and recrystallized from DMF/water to yield compounds **8a-d**.

1-[[2-[(2E)-2-benzylidenehydrazino]-6-oxo-1H-pyrimidin-5-yl] sulfonyl]-3-phenyl-thiourea(8a): Yield: 88 %; m.p.: 183–185 °C; IR (KBr) υ (cm^{-1}): 3488–3119 (NH, broad), 1676 (C=O), 1382,1177 (SO$_2$); MS (EI) *m/z*: 428 (M$^+$, 33%); ^{1}H NMR (DMSO-*d$_6$*, 300 MHz) δ (ppm): 5.20 (s, 1H, CH = N), 6.69–8.37 (m, 11*H*, Ar-H), 10.45, 10.88, 11.19, 11.48 (s, 4NH, D$_2$O exchangeable); ^{13}C NMR (DMSO, 75 MHz) δ (ppm): 51.04, 74.43 (C=N), 94.94, 110.75, 118.07, 123.21, 142.66, 151.34 (SP^2 carbon atoms), 160.63 (C=O), 165.87 (C=S); Anal. Calcd. for C$_{18}$H$_{16}$N$_6$O$_3$S$_2$ (428.07): C, 50.47; H, 3.74; N, 19.63%. Found: C, 50.47; H, 3.82; N, 19.72%.

1-[[2-[(2E)-2-benzylidenehydrazino]-6-oxo-1H-pyrimidin-5-yl] sulfonyl]-3-(4-methylphenyl)-thiourea (8b): Yield: 90 %; m.p.: 228–230 °C; IR (KBr) υ (cm^{-1}): 3474–3188 (NH, broad), 1682 (C=O), 1378,1163 (SO$_2$); MS (EI) *m/z*: 442 (M$^+$, 8.5%); ^{1}H NMR (DMSO-*d$_6$*, 300 MHz) δ (ppm): 2.31 (s, 3H, CH$_3$), 6.41 (s, 1H, CH=N), 6.76–8.12 (m, 10*H*, Ar-H), 9.82, 9.97, 10.02, 10.17 (s, 4NH, D$_2$O exchangeable); ^{13}C NMR (DMSO, 75 MHz) δ (ppm): 39.26 (CH$_3$), 52.59, 55.06 (C=N), 98.22, 104.99, 114.10, 119.57, 133.29, 140.54 (SP^2 carbon atoms), 161.93 (C=O), 175.49 (C=S); Anal. Calcd. for C$_{19}$H$_{18}$N$_6$O$_3$S$_2$ (442.09): C, 51.58; H, 4.07; N, 19.00%. Found: C, 51.41; H, 4.08; N, 19.06%.

1-[[2-[(2E)-2-benzylidenehydrazino]-6-oxo-1H-pyrimidin-5-yl] sulfonyl]-3-phenyl-urea (8c): Yield: 80 %; m.p.: 237–239 °C; IR (KBr) υ (cm^{-1}): 3484–3172 (NH, broad), 1689,1672 (2C=O), 1380,1163 (SO$_2$); MS (EI) *m/z*: 412 (M$^+$, 22.5%); ^{1}H NMR (DMSO-*d$_6$*, 300 MHz) δ (ppm): 6.72 (s, 1H, CH=N), 7.86–8.37 (m, 11*H*, Ar-H), 10.44, 10.85, 11.19, 11.49 (s, 4NH, D$_2$O exchangeable); ^{13}C NMR (DMSO, 75 MHz) δ (ppm): 51.04, 74.43 (C=N), 94.95, 125.71, 128.03, 142.66, 151.35, 152.95 (SP^2 carbon atoms), 160.64, 165.87 (C=O), Anal. Calcd. for C$_{18}$H$_{16}$N$_6$O$_4$S (412.09): C, 52.43; H, 3.88; N, 20.39%. Found: C, 52.45; H, 3.89; N, 20.46%.

1-[[2-[(2E)-2-benzylidenehydrazino]-6-oxo-1H-pyrimidin-5-yl] sulfonyl]-3-(4-methylphenyl)-urea (8d): Yield: 76 %; m.p.: >300 °C; IR (KBr) υ (cm^{-1}): 3453–3129 (NH, broad), 1688,1667 (2C=O), 1365,1159 (SO$_2$); MS (EI) *m/z*: 426 (M$^+$, 75.3%); ^{1}H NMR (DMSO-*d$_6$*, 300 MHz) δ (ppm): 2.41 (s, 3H, CH$_3$), 6.17 (s, 1H, CH=N), 6.54–8.39 (m, 10*H*, Ar-H), 10.66, 10.97, 11.16, 11.79 (s, 4NH, D$_2$O exchangeable); Anal. Calcd. for C$_{19}$H$_{18}$N$_6$O$_4$S (426.11): C, 53.52; H, 4.23; N, 19.72%. Found: C, 53.49; H, 4.09; N, 19.67%.

4.2. Biological evaluation

4.2.1. Animals

The complete course of the experiment was performed using male Wistar albino rats (200–250 g), reared and maintained in the animal house at Faculty of Pharmacy, Helwan University and provided pelleted food and water ad libitum. For acclimatization, the animals were maintained in a controlled environment of 12 h light and dark cycle for a week. The protocol of the study was approved by the animal ethics committee of Faculty of Pharmacy, Helwan University. The study was conducted in accordance with the EC, directive 86/609/EEC for animal experiments.

4.2.2. Oral toxicity study

An acute toxicity survey of the test compounds was made on albino rats following the OECD guidelines-425 [79]. Prior to the experiment, animals were fasted overnight then the test drugs were administered at the selected doses. The behavioral change was observed up to 24 h. The test compounds were found to be non-toxic at the selected doses.

4.2.3. In vivo screening of the antihyperglycemic effect of the synthesized derivatives using oral tolerance test: sucrose-loaded model (SLM)

Animals were fasted overnight. Blood samples were initially collected (0 min) and then the test derivatives were given by oral gavage to the corresponding groups (n = 6). After half an hour post-test treatment, a sucrose load of 10 gm/kg BW was given to each rat. Blood glucose levels (BGLs) were recorded at 30, 60, 90, and 120 min after sucrose load [80] using glucometer (*Gluco* Dr Super Sensor, AllMedicus Co., Ltd., Anyang, Gyeonggi, Korea) for glucose area under curve (AUC) calculation.

4.2.4. In vitro DPP-4 inhibition assay

The active compounds in SLM were screened for their DPP-4 inhibition activities as previously described [81,82] using Fluorogenic DPP-4 Assay Kit (Bps Bioscience Cornerstone Court W, Ste B San Diego, CA 92121) following the manufacturer's instructions. Test samples and linagliptin as positive control were used at concentration range from 0.01 to 10 μM and the assay was performed according to Langley *et al.* [83] and Deacon *et al.* [84].

4.2.5. Induction of type 2 diabetes mellitus in rats

Testing the antidiabetic effect of the compounds which showed promising DPP-4 inhibition was performed on diabetic rats. Hyperglycemia was induced in rats by high fat diet (HFD) that consisted of total energy 25.07 KJ/g including 60% fat, 20% protein and 20% carbohydrate for 4 weeks. Followed by an I.P. injection of streptozotocin (STZ) at a dose of 35 mg/kg (Sigma Aldrich, St. Louis, MO, USA) freshly prepared in a 0.05 M citrate buffer (pH4.5) after overnight fasting [85]. BGL was monitored after 3 days using glucometer (*Gluco* Dr Super Sensor, AllMedicus Co., Ltd., Anyang, Gyeonggi, Korea). Animals with BGL ≥ 200 mg/dL were involved in the experiment.

4.2.6. In vivo antidiabetic effect of a single dose on oral glucose tolerance test (OGTT)

Diabetic rats were randomly categorized into seven groups (6 rats/group). Animals were fasted overnight. Then, the first group orally administered vehicle only and served as T2DM control group. The rest groups orally administered linagliptin (10 mg/kg) or equivalent doses of compounds **4b, 6a, 6b, 7d** and **8b**. One hour later, all rats received an oral glucose load of 1 g/Kg. For each group, BGL was estimated at zero (before glucose load), and 30, 60, 90, and 120 min after oral administration of the glucose load using glucometer (*Gluco* Dr Super Sensor, AllMedicus Co., Ltd., Anyang, Gyeonggi, Korea).

4.2.7. Plasma DPP-4 activity in diabetic rats

To measure plasma DPP-4 activity, diabetic rats were fasted

overnight, and each group orally administered vehicle, linagliptin (10 mg/kg) or equivalent doses of compounds **4b, 6a, 6b, 7d** and **8b**. Ninety minutes after vehicle or drugs administration, blood samples were collected from the retro orbital plexus. To determine the activity of plasma DPP-4, Fluorogenic DPP-4 Assay Kit (Bps Bioscience Cornerstone Court W, Ste B San Diego, CA 92121) was used following the manufacturer's instructions.

4.2.8. Anti-inflammatory effect of the synthesized derivatives

4.2.8.1. Cell culture. RAW 264.7 macrophage cell line was obtained from the American Type Culture Collection (Manassas, VA, USA). The cells were cultured at 37 °C using DMEM (Invitrogen/Life Technologies) supplemented with 10% FBS (Hyclone, GE Healthcare, USA), 10 μg/mL of insulin, and 1% penicillin–streptomycin (Sigma-Aldrich, Saint Louis, Missouri, USA) in a humidified 5% CO_2 atmosphere.

4.2.8.2. Cell viability assay. To determine cell viability, *In Vitro* Toxicology Assay Kit, MTT Based (Sigma-Aldrich, Saint Louis, Missouri, USA) was used. Cells were plated (1.2–1.8×10^4 cells/well) at 37 °C and incubated with different concentrations of the test compounds (250, 63, 16, 4, and 1 μM) for 24 h in an incubator with 5% CO_2. At the end of the treatment, 3- [4,5- dimethylthiazol-2-yl]-2,5-diphenyl tetrazolium bromide (MTT) solution was added to each well followed by incubation at 37 °C for additional 4 h. The optical density was measured spectrophotometrically with the microplate reader (SunRise, TECAN, Inc, USA) at 590 nm. The viability of the cells was evaluated by comparing the treated cells to the non-treated ones.

4.2.8.3. Detection of Pro-Inflammatory cytokine IL-6 and CRP production. For quantification of the proinflammatory cytokines, the procedure started with seeding of RAW264.7 cells into 6-well plates (1×10^6 cells/well). When the cells reached confluence after 24 h, they were treated with concentrations equivalent to ¼ IC_{50} of the selected test compounds for 2 h. Then, 1 μg/mL of LPS was added to all treated and untreated wells to induce the inflammatory process. After 24 h, the cells were harvested for RNA extraction while the culture media were collected for ELISA analysis. The untreated wells represented the LPS control group.

4.2.8.3.1. Quantitative real-time PCR for proinflammatory cytokines analysis. Total RNA was extracted from treated RAW 264.7 cells using Qiagen RNA extraction kit (Qiagen, Germantown, MD, USA) following the manufacturer's instructions. For mRNA analysis, reverse transcription was performed using RevertAid™ H Minus Reverse Transcriptase kit (Fermentas, Thermo Fisher Scientific Inc., Canada). To quantify mRNA of *CRP* and *IL-6* expression, BioRad syber green PCR MMX was used with *CRP, IL-6,* and the housekeeping gene *ACTB* specific RT primers (Table 7). The gene transcripts were measured by quantitative real-time PCR (qPCR) using a Rotor-Gene Q (QIAGEN Hilden, Germany). All experiments were performed in triplicate. Fold change was calculated using the $2^{-\Delta\Delta Ct}$ method.

4.2.8.3.2. Measurement of cytokines by ELISA. To measure the inflammatory cytokines IL-6 and CRP in cell culture supernatants, Ab178013 Human IL-6 SimpleStep ELISA® Kit (Abcam, MA, USA) and Human C-Reactive Protein/CRP Quantikine ELISA Kit (R&D Systems, Inc., USA) were used, respectively. The assays were performed in accordance with the manufacturer's instructions.

4.2.9. Antioxidant activity (DPPH Method)

About 0.004 g DPPH reagent was dissolved in 100 mL methanol. In 96-well plates, 100 μL of the sample (50–350 μM) and 100 μL of 100 μM DPPH solution were added. The plate was incubated for 30 min at room temperature in the dark, and finally, absorbance was recorded at 595 nm wavelength. To authenticate the process, Trolox at different concentrations was used.

Table 7
Primers for mRNA.

Gene	Primers	Sequence
IL6	Forward	5′-AGACAGCCACTCACCTCTTCAG-3′
	Reverse	5′-TTCTGCCAGTGCCTCTTTGCTG-3′
CRP	Forward	5′GAACTTTCAGCCGAATACATCTTTT3′
	Reverse	5′-CCTTCCTCGACATGTCTGTCT-3′
ACTB	Forward	5′-GCACCACACCTTCTACAATG-3′
	Reverse	5′-TGCTTGCTGATCCACATCTG-3′

The degree of scavenging was calculated by the following equation: Scavenging effect (%) = [(Absorbance of control − Absorbance of sample)/Absorbance of control] × 100.

4.2.10. Statistical analysis

All data are expressed as the mean ± SD. Statistical significance was established by ANOVA using GraphPad Prism for Windows (version 5.00, GraphPad Inc, CA, USA). $p < 0.05$ was considered statistically significant. To get dose–response curves and obtain mean inhibitory concentration, IC_{50} values, we used GraphPad Prism 5.

4.3. Molecular docking

All compounds were built using **MOE 2014.09** and filed in a molecular database file [86]. The crystal structure of DPP-4 with the inhibitor was downloaded from the protein data bank (**PDB ID:2RGU**) [87]. Protein was energy minimized and 3D protonated via the structure preparation module of MOE. The complexed ligand and water molecules were removed from the crystal structure before conducting docking. The site of docking was recognized and the database containing all the tested compounds has been docked using rigid receptor as a docking protocol and triangle matcher as a placement method. London dG and GBVI/WSA dG were selected as rescoring functions and force field was used as a refinement. Free binding energy (kcal/mol) was calculated and only the best-scored pose was selected for each compound. The docked pose with the highest docking score has been selected as the most probable binding conformation of the ligand within the active site.

Declaration of Competing Interest

The authors declare that they have no known competing financial interests or personal relationships that could have appeared to influence the work reported in this paper.

Acknowledgments

Appendix A. Supplementary material

Supplementary data to this article can be found online at https://doi.org/10.1016/j.bioorg.2022.106092.

References

[1] H.A. Rasheed, H.M. Al-Kuraishy, A.I. Al-Gareeb, N.R. Hussien, M.S. Al-Nami, Effects of diabetic pharmacotherapy on prolactin hormone in patients with type 2 diabetes mellitus: bane or Boon, J Adv Pharm Technol Res 10 (4) (2019) 163–168, https://doi.org/10.4103/japtr.JAPTR_65_19.

[2] S.A. Meo, A.M. Alhowikan, T. Al-Khlaiwi, I.M. Meo, D.M. Halepoto, M. Iqbal, et al., Novel coronavirus 2019-nCoV: prevalence, biological and clinical characteristics comparison with SARS-CoV and MERS-CoV, Eur Rev Med Pharmacol Sci 24 (4) (2020) 2012–2019. https://doi.org/10.26355/eurrev_202002_20379.

[3] Ioannis Ilias, Edison Jahaj, Stylianos Kokkoris, Dimitrios Zervakis, Prodromos Temperikidis, Eleni Magira, Maria Pratikaki, A.G. Vassiliou, Christina Routsi, Anastasia Kotanidou, Ioanna Dimopoulou, Clinical study of hyperglycemia and SARS-CoV-2 infection in intensive care unit patients, In Vivo 34 (5) (2020) 3029–3032.

[4] S. Corrao, K. Pinelli, M. Vacca, M. Raspanti, C. Argano, Type 2 diabetes mellitus and COVID-19: a narrative review, Front Endocrinol (Lausanne) 12 (2021) 609470, https://doi.org/10.3389/fendo.2021.609470.

[5] R. Pranata, M.A. Lim, I. Huang, S.B. Raharjo, A.A. Lukito, Hypertension is associated with increased mortality and severity of disease in COVID-19 pneumonia: a systematic review, meta-analysis and meta-regression, 1470320320926899, J Renin Angiotens Aldosterone Syst 21 (2) (2020).

[6] S.B. Solerte, A. Di Sabatino, M. Galli, P. Fiorina, Dipeptidyl peptidase-4 (DPP4) inhibition in COVID-19, Acta Diabetol 57 (7) (2020) 779–783, https://doi.org/10.1007/s00592-020-01539-z.

[7] I. Valencia, C. Peiro, O. Lorenzo, C.F. Sanchez-Ferrer, J. Eckel, T. Romacho, DPP4 and ACE2 in diabetes and COVID-19: therapeutic targets for cardiovascular complications? Front Pharmacol 11 (2020) 1161, https://doi.org/10.3389/fphar.2020.01161.

[8] N. Vankadari, J.A. Wilce, Emerging WuHan (COVID-19) coronavirus: glycan shield and structure prediction of spike glycoprotein and its interaction with human CD26, Emerg Microbes Infect 9 (1) (2020) 601–604, https://doi.org/10.1080/22221751.2020.1739565.

[9] H.M. Al-Kuraishy, O.M. Sami, N.R. Hussain, A.I. Al-Gareeb, Metformin and/or vildagliptin mitigate type II diabetes mellitus induced-oxidative stress: the intriguing effect, J Adv Pharm Technol Res 11 (3) (2020) 142–147, https://doi.org/10.4103/japtr.JAPTR_18_20.

[10] M.F. Bassendine, S.H. Bridge, G.W. McCaughan, M.D. Gorrell, COVID-19 and comorbidities: a role for dipeptidyl peptidase 4 (DPP4) in disease severity? J Diabetes 12 (9) (2020) 649–658, https://doi.org/10.1111/1753-0407.13052.

[11] D.-S. Lee, E.-S. Lee, M.M. Alam, J.-H. Jang, H.-S. Lee, H. Oh, Y.-C. Kim, Z. Manzoor, Y.-S. Koh, D.-G. Kang, D.H. Lee, Soluble DPP-4 up-regulates toll-like receptors and augments inflammatory reactions, which are ameliorated by vildagliptin or mannose-6-phosphate, Metabolism 65 (2) (2016) 89–101, https://doi.org/10.1016/j.metabol.2015.10.002.

[12] Y. Ishibashi, T. Matsui, S. Maeda, Y. Higashimoto, S. Yamagishi, Advanced glycation end products evoke endothelial cell damage by stimulating soluble dipeptidyl peptidase-4 production and its interaction with mannose 6-phosphate/insulin-like growth factor II receptor, Cardiovasc Diabetol 12 (2013) 125, https://doi.org/10.1186/1475-2840-12-125.

[13] C.F. Deacon, Dipeptidyl peptidase 4 inhibitors in the treatment of type 2 diabetes mellitus, Nat Rev Endocrinol 16 (11) (2020) 642–653, https://doi.org/10.1038/s41574-020-0399-8.

[14] A.J. Scheen, The safety of gliptins: updated data in 2018, Exp Opin Drug Saf 17 (4) (2018) 387–405, https://doi.org/10.1080/14740338.2018.1444027.

[15] C.F. Deacon, A review of dipeptidyl peptidase-4 inhibitors. Hot topics from randomized controlled trials, Diabetes Obes Metab 20 (Suppl 1) (2018) 34–46, https://doi.org/10.1111/dom.13135.

[16] A.K. Singh, D. Yadav, N. Sharma, J.O. Jin, Dipeptidyl Peptidase (DPP)-IV inhibitors with antioxidant potential isolated from natural sources: a novel approach for the management of diabetes, Pharmaceuticals (Basel) 14 (6) (2021), https://doi.org/10.3390/ph14060586.

[17] Y. Noh, I.S. Oh, H.E. Jeong, K.B. Filion, O.H.Y. Yu, J.Y. Shin, Association Between DPP-4 Inhibitors and COVID-19-Related Outcomes Among Patients With Type 2 Diabetes, Diabetes Care 44 (4) (2021) e64–e66, https://doi.org/10.2337/dc20-1824.

[18] M. Mirani, G. Favacchio, F. Carrone, N. Betella, E. Biamonte, E. Morenghi, et al., Impact of comorbidities and glycemia at admission and dipeptidyl peptidase 4 inhibitors in patients with type 2 diabetes With COVID-19: a case series from an academic hospital in Lombardy, Italy, Diabetes Care 43 (12) (2020) 3042–3049, https://doi.org/10.2337/dc20-1340.

[19] M.A. Abu-Zaied, G.H. Elgemeie, N.M. Mahmoud, Anti-covid-19 drug analogues: synthesis of novel pyrimidine thioglycosides as antiviral agents against SARS-COV-2 and avian influenza H5N1 viruses, ACS Omega 6 (26) (2021) 16890–16904, https://doi.org/10.1021/acsomega.1c01501.

[20] P. Mehta, D.F. McAuley, M. Brown, E. Sanchez, R.S. Tattersall, J.J. Manson, et al., COVID-19: consider cytokine storm syndromes and immunosuppression, Lancet 395 (10229) (2020) 1033–1034, https://doi.org/10.1016/S0140-6736(20)30628-0.

[21] K. Tomovic, B.S. Ilic, A. Smelcerovic, Structure-activity relationship analysis of cocrystallized gliptin-like pyrrolidine, trifluorophenyl, and pyrimidine-2,4-dione dipeptidyl peptidase-4 inhibitors, J Med Chem 64 (14) (2021) 9639–9648, https://doi.org/10.1021/acs.jmedchem.1c00203.

[22] S. Arulmozhiraja, N. Matsuo, E. Ishitsubo, S. Okazaki, H. Shimano, H. Tokiwa, Comparative binding analysis of dipeptidyl peptidase IV (DPP-4) with antidiabetic drugs - an ab initio fragment molecular orbital study, PLoS ONE 11 (11) (2016) 1–15, https://doi.org/10.1371/journal.pone.0166275.

[23] S. Roppongi, Y. Suzuki, C. Tateoka, M. Fujimoto, S. Morisawa, I. Iizuka, et al., Crystal structures of a bacterial dipeptidyl peptidase IV reveal a novel substrate recognition mechanism distinct from that of mammalian orthologues, Sci Rep 8 (1) (2018) 1–5, https://doi.org/10.1038/s41598-018-21056-y.

[24] M. Nabeno, F. Akahoshi, H. Kishida, I. Miyaguchi, Y. Tanaka, S. Ishii, et al., A comparative study of the binding modes of recently launched dipeptidyl peptidase IV inhibitors in the active site, Biochem Biophys Res Commun 434 (2) (2013) 191–196, https://doi.org/10.1016/j.bbrc.2013.03.010.

[25] N.H. Kim, T. Yu, D.H. Lee, The nonglycemic actions of dipeptidyl peptidase-4 inhibitors, BioMed Res Int 2014 (2014), https://doi.org/10.1155/2014/368703.

[26] Y. Ohara-Nemoto, S.M.A. Rouf, M. Naito, A. Yanase, F. Tetsuo, T. Ono, et al., Identification and characterization of prokaryotic dipeptidyl-peptidase 5 from porphyromonas gingivalis, J Biol Chem 289 (9) (2014) 5436–5448, https://doi.org/10.1074/jbc.M113.527333.

[27] Y. Ohara-Nemoto, Y. Shimoyama, T. Ono, M.T. Sarwar, M. Nakasato, M. Sasaki, et al., Expanded substrate specificity supported by P10 and P20 residues enables bacterial dipeptidyl-peptidase 7 to degrade bioactive peptides, J Biol Chem 298 (3) (2022) 101585, https://doi.org/10.1016/j.jbc.2022.101585.

[28] T.K. Nemoto, Y. Ohara Nemoto, Dipeptidyl-peptidases: key enzymes producing entry forms of extracellular proteins in asaccharolytic periodontopathic bacterium Porphyromonas gingivalis, Mole Oral Microbiol 36 (2) (2021) 145–156.

[29] R. Thoma, B. Löffler, M. Stihle, W. Huber, A. Ruf, M. Hennig, Structural basis of proline-specific exopeptidase activity as observed in human dipeptidyl peptidase-IV, Structure 11 (8) (2003) 947–959, https://doi.org/10.1016/S0969-2126(03)00160-6.

[30] C.H. Wilson, H.E. Zhang, M.D. Gorrell, C.A. Abbott, Dipeptidyl peptidase 9 substrates and their discovery: current progress and the application of mass spectrometry-based approaches, Biol Chem 397 (9) (2016) 837–856, https://doi.org/10.1515/hsz-2016-0174.

[31] T. Murai, Chem Thioamid (2019).

[32] M. Kawakubo, M. Tanaka, K. Ochi, A. Watanabe, M. Saka-Tanaka, Y. Kanamori, et al., Dipeptidyl peptidase-4 inhibition prevents nonalcoholic steatohepatitis–associated liver fibrosis and tumor development in mice independently of its anti-diabetic effects, Sci Rep 10 (1) (2020) 1–11, https://doi.org/10.1038/s41598-020-57935-6.

[33] P.K. Huang, S.R. Lin, C.H. Chang, M.J. Tsai, D.N. Lee, C.F. Weng, Natural phenolic compounds potentiate hypoglycemia via inhibition of Dipeptidyl peptidase IV, Sci Rep 9 (1) (2019) 1–11, https://doi.org/10.1038/s41598-019-52088-7.

[34] T. Karagiannis, P. Boura, A. Tsapas, Safety of dipeptidyl peptidase 4 inhibitors: a perspective review, Therapeut Adv Drug Safety 5 (3) (2014) 138–146, https://doi.org/10.1177/2042098614523031.

[35] N.N. Ta, C.A. Schuyler, Y. Li, M.F. Lopes-Virella, Y. Huang, DPP-4 (CD26) inhibitor alogliptin inhibits atherosclerosis in diabetic apolipoprotein E-deficient mice, J Cardiovasc Pharmacol 58 (2) (2011) 157–166, https://doi.org/10.1097/FJC.0b013e31821e5626.

[36] A. Soare, H.A. Györfi, A.E. Matei, C. Dees, S. Rauber, T. Wohlfahrt, et al., Dipeptidylpeptidase 4 as a marker of activated fibroblasts and a potential target for the treatment of fibrosis in systemic sclerosis, Arthrit Rheumatol 72 (1) (2020) 137–149, https://doi.org/10.1002/art.41058.

[37] A.A.E. Mourad, A.E. Khodir, S. Saber, M.A.E. Mourad, Novel potent and selective DPP-4 inhibitors: design, synthesis and molecular docking study of dihydropyrimidine phthalimide hybrids, Pharmaceuticals 14 (2) (2021) 1–24, https://doi.org/10.3390/ph14020144.

[38] A. Fathalla, W.A. Zaghary, H.H. Radwan, S.M. Awad, M.S. Mohamed, Synthesis of new 2-thiouracil-5-sulfonamide derivatives with biological activity, Arch Pharm Res 25 (3) (2002) 258–269, https://doi.org/10.1007/BF02976623.

[39] S.W. Ahjel, S.M. Hassan, S.F. Hussein, N.R. Hadi, S.M. Awad, Antineoplastic effect of new synthesized compounds of 2-thiouracil sulfonamide derivatives against ovarian and breast carcinoma cells "In Vitro Study", System Rev Pharm 11 (4) (2020) 229–237, https://doi.org/10.31838/srp.2020.4.33.

[40] S. Kang, M. Watanabe, J.C. Jacobs, M. Yamaguchi, S. Dahesh, V. Nizet, et al., Synthesis of mevalonate- and fluorinated mevalonate prodrugs and their in vitro human plasma stability, Eur J Med Chem 90 (2015) 448–461, https://doi.org/10.1016/j.ejmech.2014.11.040.

[41] J. Klenc, E. Raux, S. Barnes, S. Sullivan, B. Duszynska, A.J. Bojarski, et al., Synthesis of 4-substituted 2-(4-methylpiperazino) pyrimidines and quinazoline analogs as serotonin 5-HT 2A receptor ligands, J Heterocycl Chem 46 (November) (2009) 1259–1265, https://doi.org/10.1002/jhet.

[42] M. Barmaki, G. Valiyeva, A.A. Maharramovm, M.M. Allaverdiyev, Synthesis of 2,3-dihydro-6-methyl-2-thiopyrimidin-4(1h)-one (6-methylthiouracil) derivatives and their reactions, J Chem (2013).

[43] A.F. Eweas, Q.M.A. Abdallah, E.S.I. Hassan, Design, synthesis, molecular docking of new thiopyrimidine-5-carbonitrile derivatives and their cytotoxic activity against HepG2 cell line, J Appl Pharm Sci 4 (12) (2014) 102–111.

[44] F.A. Attaby, S.M. Eldin, E.A.Z. Hanafi, Reactions of pyrimidinonethione derivatives: Synthesis of 2-hydrazinopyrimidin-4-one, pyrimido[1,2-a]-1,2,4-triazine, triazolo-[1,2-a]pyrimidine, 2-(1-pyrazolo)pyrimidine and 2-arylhydrazonopyrimidine derivatives, Arch Pharmacal Res 20 (6) (1997) 620–628, https://doi.org/10.1007/BF02975221.

[45] M.A.B. Khan, M.J. Hashim, J.K. King, R.D. Govender, H. Mustafa, J. Al Kaabi, Epidemiology of type 2 diabetes - global burden of disease and forecasted trends, J Epidemiol Glob Health 10 (1) (2020) 107–111.

[46] R.K. Campbell, Fate of the beta-cell in the pathophysiology of type 2 diabetes, J Am Pharm Assoc (2003) 49 (Suppl 1) (2009) S10–S15.

[47] P.N. Surampudi, J. John-Kalarickal, V.A. Fonseca, Emerging concepts in the pathophysiology of type 2 diabetes mellitus, Mt Sinai J Med 76 (3) (2009) 216–226, https://doi.org/10.1002/msj.20113.

[48] A.A. Al-Atram, A review of the bidirectional relationship between psychiatric disorders and diabetes mellitus, Neurosciences (Riyadh) 23 (2) (2018) 91–96, https://doi.org/10.17712/nsj.2018.2.20170132.

[49] T. Sozen, N.C. Basaran, M. Tinazli, L. Ozisik, Musculoskeletal problems in diabetes mellitus, Eur J Rheumatol 5 (4) (2018) 258–265, https://doi.org/10.5152/eurjrheum.2018.18044.

[50] B.M. Leon, T.M. Maddox, Diabetes and cardiovascular disease: Epidemiology, biological mechanisms, treatment recommendations and future research, World J Diabetes 6 (13) (2015) 1246–1258, https://doi.org/10.4239/wjd.v6.i13.1246.

[51] G. Targher, A. Mantovani, X.B. Wang, H.D. Yan, Q.F. Sun, K.H. Pan, et al., Patients with diabetes are at higher risk for severe illness from COVID-19, Diabetes Metab 46 (4) (2020) 335–337, https://doi.org/10.1016/j.diabet.2020.05.001.

[52] A.K. Singh, K. Khunti, Assessment of risk, severity, mortality, glycemic control and antidiabetic agents in patients with diabetes and COVID-19: A narrative review, Diabetes Res Clin Pract 165 (2020) 108266, https://doi.org/10.1016/j.diabres.2020.108266.

[53] S.W. Lim, J.Z. Jin, L. Jin, J. Jin, C. Li, Role of dipeptidyl peptidase-4 inhibitors in new-onset diabetes after transplantation, Korean J Int Med 30 (6) (2015) 759–770, https://doi.org/10.3904/kjim.2015.30.6.759.

[54] E. Maddaloni, R. Buzzetti, Covid-19 and diabetes mellitus: unveiling the interaction of two pandemics, Diabetes Metab Res Rev (2020) e33213321, https://doi.org/10.1002/dmrr.3321.

[55] E.E. Mulvihill, D.J. Drucker, Pharmacology, physiology, and mechanisms of action of dipeptidyl peptidase-4 inhibitors, Endocr Rev 35 (6) (2014) 992–1019, https://doi.org/10.1210/er.2014-1035.

[56] Y. Waumans, L. Baerts, K. Kehoe, A.M. Lambeir, I. De Meester, The dipeptidyl peptidase family, prolyl oligopeptidase, and prolyl carboxypeptidase in the immune system and inflammatory disease, including atherosclerosis, Front Immunol 6 (2015) 387, https://doi.org/10.3389/fimmu.2015.00387.

[57] F. Zhuge, Y. Ni, M. Nagashimada, N. Nagata, L. Xu, N. Mukaida, et al., DPP-4 inhibition by linagliptin attenuates obesity-related inflammation and insulin resistance by regulating M1/M2 macrophage polarization, Diabetes 65 (10) (2016) 2966–2979, https://doi.org/10.2337/db16-0317.

[58] K. Michalakis, I. Ilias, SARS-CoV-2 infection and obesity: Common inflammatory and metabolic aspects, Diabetes Metab Syndr 14 (4) (2020) 469–471, https://doi.org/10.1016/j.dsx.2020.04.033.

[59] H. Al-Kuraishy, T. Al-Maiahy, A. Al-Gareeb, R. Musa, Z. Ali, COVID-19 pneumonia in an Iraqi pregnant woman with preterm delivery, Asian Pacific J Reprod 9 (3) (2020), https://doi.org/10.4103/2305-0500.282984.

[60] S.F. Pedersen, Y.C. Ho, SARS-CoV-2: a storm is raging, J Clin Invest 130 (5) (2020) 2202–2205, https://doi.org/10.1172/JCI137647.

[61] A.A. Al-Qahtani, K. Lyroni, M. Aznaourova, M. Tseliou, M.R. Al-Anazi, M.N. Al-Ahdal, et al., Middle east respiratory syndrome corona virus spike glycoprotein suppresses macrophage responses via DPP4-mediated induction of IRAK-M and PPARgamma, Oncotarget 8 (6) (2017) 9053–9066. https://doi.org/10.18632/oncotarget.14754.

[62] T. Kawasaki, W. Chen, Y.M. Htwe, K. Tatsumi, S.M. Dudek, DPP4 inhibition by sitagliptin attenuates LPS-induced lung injury in mice, Am J Physiol Lung Cell Mol Physiol 315 (5) (2018) L834–L845, https://doi.org/10.1152/ajplung.00031.2018.

[63] J. Xu, J. Wang, M. He, H. Han, W. Xie, H. Wang, et al., Dipeptidyl peptidase IV (DPP-4) inhibition alleviates pulmonary arterial remodeling in experimental pulmonary hypertension, Lab Invest 98 (10) (2018) 1333–1346, https://doi.org/10.1038/s41374-018-0080-1.

[64] Y.S. Lee, M.S. Park, J.S. Choung, S.S. Kim, H.H. Oh, C.S. Choi, et al., Glucagon-like peptide-1 inhibits adipose tissue macrophage infiltration and inflammation in an obese mouse model of diabetes, Diabetologia 55 (9) (2012) 2456–2468, https://doi.org/10.1007/s00125-012-2592-3.

[65] Y.S. Lee, H.S. Jun, Anti-inflammatory effects of GLP-1-based therapies beyond glucose control, Mediat Inflamm 2016 (2016) 3094642, https://doi.org/10.1155/2016/3094642.

[66] J. Wu, M. Li, L. Liu, Q. An, J. Zhang, J. Zhang, et al., Nitric oxide and interleukins are involved in cell proliferation of RAW264.7 macrophages activated by viili exopolysaccharides, Inflammation 36 (4) (2013) 954–961.

[67] L. Dong, L. Yin, Y. Zhang, X. Fu, J. Lu, Anti-inflammatory effects of ononin on lipopolysaccharide-stimulated RAW 264.7 cells, Mol Immunol 83 (2017) 46–51, https://doi.org/10.1016/j.molimm.2017.01.007.

[68] L.B. Zhang, Z.T. Man, W. Li, W. Zhang, X.Q. Wang, S. Sun, Calcitonin protects chondrocytes from lipopolysaccharide-induced apoptosis and inflammatory response through MAPK/Wnt/NF-kappaB pathways, Mol Immunol 87 (2017) 249–257, https://doi.org/10.1016/j.molimm.2017.05.002.

[69] K. Muniandy, S. Gothai, K.M.H. Badran, S. Suresh Kumar, N.M. Esa, P. Arulselvan, Suppression of proinflammatory cytokines and mediators in LPS-induced RAW 264.7 macrophages by stem extract of alternanthera sessilis via the inhibition of the NF-kappaB pathway, J Immunol Res (2018) 3430684, https://doi.org/10.1155/2018/3430684.

[70] M. Eckhardt, E. Langkopf, M. Mark, M. Tadayyon, L. Thomas, H. Nar, et al., 8-(3-(R)-aminopiperidin-1-yl)-7-but-2-ynyl-3-methyl-1-(4-methyl-quinazolin-2-ylmethyl)-3,7-dihydropurine-2,6-dione (BI 1356), a highly potent, selective, long-acting, and orally bioavailable DPP-4 inhibitor for the treatment of type 2 diabetes, J Med Chem 50 (26) (2007) 6450–6453, https://doi.org/10.1021/jm701280z.

[71] E. Molecular Operating, Chemical Computing Group ULC, 1010 Sherbrooke St. West, Suite# 910; 2016.

[72] P. Kalhotra, V. Chittepu, G. Osorio-Revilla, T. Gallardo-Velazquez, Structure(-) activity relationship and molecular docking of natural product library reveal chrysin as a novel dipeptidyl peptidase-4 (DPP-4) inhibitor: an integrated in silico and in vitro study, Molecules 23 (6) (2018), https://doi.org/10.3390/molecules23061368.

[73] H. Zettl, M. Schubert-Zsilavecz, D. Steinhilber, Medicinal chemistry of incretin mimetics and DPP-4 inhibitors, ChemMedChem 5 (2) (2010) 179–185, https://doi.org/10.1002/cmdc.200900448.

[74] K. Aertgeerts, Crystal structure of human dipeptidyl peptidase IV in complex with a decapeptide reveals details on substrate specificity and tetrahedral intermediate formation, Protein Sci 13 (2) (2004) 412–421, https://doi.org/10.1110/ps.03460604.

[75] J.P. Berger, R. SinhaRoy, A. Pocai, T.M. Kelly, G. Scapin, Y.-D. Gao, et al., A comparative study of the binding properties, dipeptidyl peptidase-4 (DPP-4) inhibitory activity and glucose-lowering efficacy of the DPP-4 inhibitors alogliptin, linagliptin, saxagliptin, sitagliptin and vildagliptin in mice, Endocrinol Diabet Metab 1 (1) (2018) e00002, https://doi.org/10.1002/edm2.2.

[76] H. Nojima, K. Kanou, G. Terashi, M. Takeda-Shitaka, G. Inoue, K. Atsuda, et al., Comprehensive analysis of the co-structures of dipeptidyl peptidase IV and its inhibitor, BMC Struct Biol 16 (1) (2016) 1–14, https://doi.org/10.1186/s12900-016-0062-8.

[77] M.F. El-Shehry, K.M. Abu-Zied, E.F. Ewies, S.M. Awad, M.E. Mohram, Synthesis of some novel azaheterocycles utilizing 3-(4-nitrobenzylidene)-5-phenylfuran-2 (3h)-one with expected antimicrobial activity, Der pharma Chem 5 (5) (2013) 318–326.

[78] S.M. Hassan, A.N.A. Al-Jaf, Y.A. Hussien, S.M. Awad, M.A. Abdulkhaleq, N.R. Hadi, Effect of new synthesized compounds of 2-thiouracil sulfonamide derivatives against colon and liver carcinoma cells "in vitro study", Int J Pharm Res 12 (4) (2020) 2012–2016. https://doi.org/10.31838/ijpr/2020.12.04.286.

[79] OECD, Test No 425: Acute Oral Toxicity: Up-and-Down Procedure, OECD Guidelines for the Testing of Chemicals, Section 4 (2008) 1-27. https://doi.org/10.1787/9789264071049-en.

[80] F.V. Singh, A. Parihar, S. Chaurasia, A.B. Singh, S.P. Singh, A.K. Tamrakar, et al., 5,6-Diarylanthranilo-1,3-dinitriles as a new class of antihyperglycemic agents, Bioorg Med Chem Lett 19 (8) (2009) 2158–2161, https://doi.org/10.1016/j.bmcl.2009.02.118.

[81] S. Li, H. Xu, S. Cui, F. Wu, Y. Zhang, M. Su, et al., Discovery and rational design of natural-product-derived 2-phenyl-3,4-dihydro-2H-benzo[f]chromen-3-amine analogs as novel and potent dipeptidyl peptidase 4 (DPP-4) inhibitors for the treatment of type 2 diabetes, J Med Chem 59 (14) (2016) 6772–6790, https://doi.org/10.1021/acs.jmedchem.6b00505.

[82] X. Ji, M. Su, J. Wang, G. Deng, S. Deng, Z. Li, et al., Design, synthesis and biological evaluation of hetero-aromatic moieties substituted pyrrole-2-carbonitrile derivatives as dipeptidyl peptidase IV inhibitors, Eur J Med Chem 75 (2014) 111–122, https://doi.org/10.1016/j.ejmech.2014.01.021.

[83] A.K. Langley, T.J. Suffoletta, H.R. Jennings, Dipeptidyl peptidase IV inhibitors and the incretin system in type 2 diabetes mellitus, Pharmacotherapy 27 (8) (2007) 1163–1180, https://doi.org/10.1592/phco.27.8.1163.

[84] C.F. Deacon, R.D. Carr, J.J. Holst, DPP-4 inhibitor therapy: new directions in the treatment of type 2 diabetes, Front Biosci 13 (2008) 1780–1794, https://doi.org/10.2741/2799.

[85] K. Srinivasan, B. Viswanad, L. Asrat, C.L. Kaul, P. Ramarao, Combination of high-fat diet-fed and low-dose streptozotocin-treated rat: a model for type 2 diabetes and pharmacological screening, Pharmacol Res 52 (4) (2005) 313–320, https://doi.org/10.1016/j.phrs.2005.05.004.

[86] Ulc CCG. Molecular Operating Environment (MOE), 2013.08, 1010 Sherbooke St. West, Suite# 910, Montreal, QC, Canada, H3A 2R7 10; 2018.

[87] M. Eckhardt, E. Langkopf, M. Mark, M. Tadayyon, L. Thomas, H. Nar, et al., 8-(3-(R)-aminopiperidin-1-yl)-7-but-2-ynyl-3-methyl-1-(4-methyl-quinazolin-2-ylmethyl)-3, 7-dihydropurine-2, 6-dione (BI 1356), a highly potent, selective, long-acting, and orally bioavailable DPP-4 inhibitor for the treatment of type 2 diabetes, J Med Chem 50 (26) (2007) 6450–6453.